1 <u>(Accepted version, post peer review and revisions)</u>

2

Quantifying brine assimilation by submarine magmas:

examples from the Galápagos Spreading Centre and Lau

Basin

6

7

8 Mark A. Kendrick[1*], Richard Arculus[2], Pete Burnard[3], Masahiko Honda[2]

9

10

11   1- School of Earth Sciences, University of Melbourne, Victoria 3010, Australia

12   2- Research Schoo of Earth Sciences, Australian National University, ACT 0200,

13 Australia.

14 3- CRPG, CNRS, Nancy, France.

15 *Corresponding Author: mark.kendrick@unimelb.edu.au ;

16   Tel +61 3 8344 6933; Fax +61 3 8344 7761

17

20

Abstract. Volatiles are critically important in controlling the chemical and physical properties of the mantle. However, determining mantle volatile abundances via the preferred proxy of submarine volcanic glass can be hampered by seawater assimilation. This study shows how combined Cl, Br, I, K and H_2O abundances can be used to unambiguously constrain the dominant mechanism by which melts assimilate seawater-derived components, and provide an improved method for determining mantle H_2O and Cl abundances. We demonstrate that melts from the northwest part of the Lau Basin, the Galápagos Spreading Centre and melts from other locations previously shown to have anomalously high Cl contents, all assimilated excess Cl and H_2O from ultra-saline brines with estimated salinities of 55 ± 15 wt. % salts. Assimilation probably occurs at depths of ~3-6 km in the crust when seawater-derived fluids come into direct contact with deep magmas. In addition to their ultra-high salinity, the brines are characterised by K/Cl of <0.2, I/Cl of close to the seawater value (~3×10^{-6}) and distinctive Br/Cl ratios of $3.7-3.9\times10^{-3}$, that are higher than both the seawater value of 3.5×10^{-3} and the range of Br/Cl in 43 pristine E-MORB and OIB glasses that are considered representative of diverse mantle reservoirs [Br/Cl$_{mantle}$ = $(2.8 \pm 0.6)\times10^{-3}$ and I/Cl$_{mantle}$ = $(60 \pm 30)\times10^{-6}$ (2σ)]. The ultra-saline brines, with characteristically elevated Br/Cl ratios, are produced by a combination of fluid-rock reactions during crustal hydration and hydrothermal boiling. The relative importance of these processes is unknown; however, it is envisaged that a vapour phase will be boiled off when crustal fluids are heated to magmatic temperatures during assimilation. Furthermore, the ultra-high salinity of the residual brine that is assimilated may be partly determined by the relative solubilities of H_2O and Cl in basaltic melts. The most contaminated glasses from the Galápagos Spreading Centre and Lau Basin have assimilated ~95 % of their total Cl and 35-40 % of their total H_2O, equivalent to the melts assimilating 1000-2000 ppm brine at an early stage of their evolution. Dacite glasses from Galapagos contain even higher concentrations of brine components (e.g. 12,000 ppm), but the H_2O and Cl in these melts was probably concentrated by fractional crystallisation after assimilation. The Cl, Br, I and K data presented here confirm the proportion of seawater-derived volatiles assimilated by submarine magmas can vary from zero to nearly 100 %, and that assimilation is closely related to hydrothermal activity. Assimilation of seawater components has previously been recognised as a possible source of atmospheric noble gases in basalt glasses. However, hydrothermal brines have

52 metal and helium concentrations up to hundreds of times greater than seawater, and brine

53 assimilation could also influence the helium isotope systematics of some submarine glasses.

54

Introduction

Magmatic volatile components that exsolve into supercritical fluids or gases include H_2O, CO_2, halogens, S, N and noble gases. The major volatiles exert important controls on the physical properties of mantle minerals, mantle solidus temperatures, melt viscosity and influence the style of volcanic eruptions (e.g. Carroll and Holloway, 1994; Filiberto and Treiman, 2009; Litasov et al., 2006). The trace volatiles, especially iodine and noble gases, are powerful markers that can potentially constrain the distribution of recycled versus primordial volatile components within the Earth's mantle (Deruelle et al., 1992; Graham, 2002; Hilton and Porcelli, 2003; Kendrick et al., 2012a). The volatile contents of basaltic glasses from different tectonic settings (e.g. mid-ocean ridge, back arc and oceanic island) are therefore of great interest, but relating the measured concentrations of volatiles in basaltic glasses to mantle abundances is challenging.

The least soluble volatiles (CO_2 and noble gases) are degassed from erupting lavas and as a result only melt inclusions trapped within deep magma chambers record pre-eruptive CO_2 concentrations, and noble gases occur dominantly in CO_2 vesicles (Burnard et al., 2002; Graham, 2002; Saal et al., 2002). In contrast, H_2O and halogens have much higher solubilities in basaltic melts, and halogens appear to be retained in melts erupted in water depths of greater than ~500 m (Straub and Layne, 2003; Unni and Schilling, 1978). Nonetheless seawater assimilation can be a potentially serious obstacle to determining the primary mantle source characteristic of halogens, H_2O and any other volatile that has a high abundance in seawater and a comparatively low abundance in mantle-derived melt (e.g. Fisher, 1997; Graham, 2002; Kent et al., 1999ab; 2002; Michael and Cornell, 1998; Michael and Schilling, 1989; Patterson et al., 1990).

Numerous studies have demonstrated that atmospheric noble gases (Ne, Ar, Kr, Xe) are a distinctive and ubiquitous component within basalt glasses (e.g. Graham, 2002; Hilton

and Porcelli, 2003). It is likely that some fraction of these atmospheric noble gases are introduced by seawater assimilation processes (e.g. Patterson et al., 1990); however, atmospheric noble gases could also be introduced during sample preparation (Ballentine and Barfod, 2000), or they could be present as a recycled component within the mantle (Bach and Niedermann, 1998; Sarda, 2004).

In contrast to noble gases, assimilation of Cl is associated with seafloor hydrothermal activity and while it has been documented in Hawaii (Coombs et al., 2004; Kent et al., 1999ab) and some fast spreading centres (le Roux et al., 2006), it is uncommon in basalts generated at slow spreading centres (Michael and Cornell, 1998; Michael and Schilling, 1989). Improving constraints on the spatially limited assimilation processes affecting Cl concentrations has implications for the origin of atmospheric noble gases in basalt glasses, and igneous petrology. Assimilation accelerates volatile saturation and triggers exsolution of fluid phases meaning it can cause rapid crystallisation of magmas and critically influence the way oceanic crust accretes (Coogan et al., 2003; Perfit et al., 2003; Soule et al., 2006). Furthermore, it has been proposed that partial melting of seawater-altered oceanic crust contributes to the petrogenesis of silicic mid-ocean ridge lavas such as dacites (Wanless et al., 2010; 2011).

The assimilated components proposed in previous Cl studies have poorly defined but high Cl/H_2O ratios that preclude the direct involvement of seawater and favour a role for brines with salinities of ~10-50 wt % salts, or Cl-rich minerals formed by seawater alteration (Kent et al., 1999ab; 2002; le Roux et al., 2006; Michael and Schilling, 1989; Perfit et al., 1999; Wanless et al., 2010; 2011). This study extends the previous analyses to include Br and I in 19 glasses that have assimilated varying proportions of seawater-derived volatiles and sample different parts of the Earth's mantle. We show how multi-component correlations between Cl, Br, I, K and H_2O can be used to rigorously test the nature of

105   seawater assimilation, and quantify the proportions of seawater-derived halogens and H_2O in

106   basalt glass. In addition, we refine previous estimates of mantle Br/Cl and I/Cl by re-

107   examining standardisation (Kendrick et al., 2012ab) thereby providing improved agreement

108   with earlier halogen studies (Jambon et al., 1995; Schilling et al., 1978; 1980), and

109   demonstrating fairly limited variation of Br/Cl and I/Cl in the Earth's mantle.

110

1.1 Samples

112   Pristine basalt glasses were selected from a range of seafloor settings with varying

113   exposure to assimilation processes. Enriched mid-ocean ridge basalt (E-MORB) glasses

114   defined as having primitive mantle normalised $(La/Sm)_N$ of >1 were selected from the Mid-

115   Atlantic Ridge at the Famous location (36° 50' N) and the popping rock area (13° 50' N)

116   (Bryan et al., 1979; Bougault et al., 1988; Langmuir et al., 1977). These samples were

117   expected to preserve pristine mantle halogen signatures because E-MORB have high

118   concentrations of incompatible trace elements and assimilation of Cl is asserted to be a minor

119   artefact for E-MORB formed at slow spreading ridges (Michael and Cornell, 1998).

120   Furthermore, the popping rock sample 2πD43 is famous for its uniquely good preservation of

121   mantle noble gas signatures (e.g. Moreira et al., 1998; Mukhopadhyay, 2012), which suggest

122   it is very unlikely to have assimilated significant seawater-derived H_2O or Cl during

123   emplacement (cf. Ballentine and Barfod, 2000; Burnard et al., 1997; Moreira et al., 1998;

124   Sarda, 2004; Staudacher et al., 1989; Trieloff et al., 2003).

125   Samples expected to show the effects of seawater contamination comprise: basalt and

126   dacite glasses recovered from 0° 50' N from the Galápagos Spreading Centre during Alvin

127   dive 1652, that investigated an area of crust exhibiting particularly extensive hydrothermal

128   alteration (Embley et al., 1988); and N-MORB samples from the southern Juan de Fuca

129 Ridge where there is also significant hydrothermal activity (45-46° N; Smith et al., 1994).

130 Additional N-MORB, which are defined as having $(La/Sm)_N$ of <1, were available for

131 locations on the East Pacific Rise (12° 46' N; Hekinian et al., 1983) and Mid-Atlantic Ridge

132 (30-32° N; Bougault and Treuil, 1980). The Galápagos glasses recovered during Alvin dive

133 1652 are pristine but have been shown to exhibit traces of seawater assimilation (Michael and

134 Cornell, 1998; Perfit et al., 1999). N-MORB samples were selected from the other locations

135 because their generally low Cl content renders them more susceptible to seawater

136 assimilation than Cl-rich E-MORB (Michael and Cornell, 1998), although the high $^{40}Ar/^{36}Ar$

137 ratio of sample CH98-DR11 (>25,000) suggests minimal assimilation in this case (Marty and

138 Humbert, 1997).

139 As a contrast to the variably enriched MORB samples, five glasses were selected from

140 the northwest Lau Basin (14-16° S; Lupton et al., 2009), primarily because of their high

141 $^{3}He/^{4}He$ ratios of 12-28 Ra (where Ra is the atmospheric $^{3}He/^{4}He$ ratio of $1.4×10^{-6}$) and neon

142 isotope signatures that are typical of primitive mantle sampled by some ocean island basalts

143 (OIB; Lupton et al., 2009; 2012). Despite the unusual $^{3}He/^{4}He$ signatures, the trace element

144 abundances of these glasses are fairly typical of MORB [$(La/Sm)_N$ of 0.4-1.2], and they lack

145 evidence for slab-derived subduction components (Lytle et al., 2012). These glasses were

146 however of additional interest because the effects of seawater assimilation have been

147 previously documented elsewhere in the Lau Basin (Kent et al., 2002).

148

149 **2. Methods and halogen standardisation**

150 The majority of samples included in this study were characterised using a range of

151 techniques during the 1970's and 80's, and re-analysed at the University of Melbourne using

152 a Cameca SX-50 electron microprobe for major elements and laser ablation system coupled

153 to an Agilent 7700x inductively-coupled plasma mass spectrometer (ICP-MS) for trace

154 elements (supplementary information). In contrast, ICP-MS was used to analyse trace

155 elements in solutions formed by dissolving 50 mg sized aliquots of the Famous samples.

156 Chlorine measurements by electron microprobe had a detection limit of ~85 ppm and were

157 standardised using Durango apatite (0.41 wt % Cl) and scapolite (1.43 wt % Cl;

158 supplementary information).

159 Simultaneous Cl, Br, I and K measurements were achieved via the noble gas method

160 (Kendrick, 2012). Samples of ~10-30 mg comprising pristine glass chips (0.2-1 mm in size)

161 were wrapped in Al-foil, placed in an irradiation canister, and irradiated in position 5c of the

162 McMaster Nuclear Reactor, Canada (irradiations UM#44: 42 hrs on 27/02/2011 received 10^{19}

163 neutrons cm^{-2}; thermal/fast = 2.7; and UM#48: 30 hrs on 15/12/2011 received 8×10^{18}

164 neutrons cm^{-2}; thermal/fast = 2.7). Irradiation-produced noble gas proxy isotopes ($^{38}Ar_{Cl}$,

165 $^{80}Kr_{Br}$ $^{128}Xe_I$ and $^{39}Ar_K$) were then extracted from the samples by furnace heating and

166 measured on the MAP-215 noble gas mass spectrometer at the University of Melbourne. It

167 was found that gas released from 10 mg sized samples at 300 °C was at the blank level, and

168 the majority of samples were therefore preheated to 300 °C before extraction of halogen-

169 derived noble gas isotopes in a single 1500 °C step of 20 minutes duration. Small blank

170 corrections amounted to <1% of the sample gas and the abundances of noble gas proxy

171 isotopes ($^{38}Ar_{Cl}$, $^{80}Kr_{Br}$ $^{128}Xe_I$ and $^{39}Ar_K$), determined by comparison to an air standard, were

172 converted to Cl, Br, I and K on the basis of production ratios monitored with Hb3Gr and

173 scapolite halogen standards (Fig 1; Kendrick, 2012).

174 The noble gas method has significant advantages over radiochemical neutron

175 activation analyses used in previous Br and I studies of basalt glass (Deruelle et al., 1992;

176 Jambon et al., 1995; Schilling et al., 1978; Schilling et al., 1980): 1.) chemical separation of

177 halogens is not required which avoids the possibility of fractionating halogen abundance

178   ratios during extraction; 2.) very high sensitivity and low detection limits mean it can be

179   applied to small samples and it is therefore easier to obtain high purity glass separates; and

180   3.) it has very high internal precision of ~2-4% (2σ), compared to ~20-40% (2σ) in previous

181   studies (Deruelle et al., 1992; Jambon et al., 1995; Schilling et al., 1978; 1980; Unni and

182   Schilling, 1977). Nonetheless, the external precision (or accuracy) of the method is dependent

183   on the availability of well characterised halogen standards and some refinements to the Br

184   and I abundances in the scapolite standards used by Kendrick et al. (2012ab) have proven

185   necessary (Kendrick et al., 2013).

186   The Br/Cl and I/Cl ratios now recommended for the standards (Fig 1) are considered

187   superior to the original values (Kendrick, 2012) because they are independent of the Bjurbole

188   meteorite standard, and they provide improved agreement with other techniques (Table S5;

189   supplementary information; Hammerli et al., 2013). Adoption of the new standard values

190   (Fig 1) means revising previously reported Br and I abundances (Kendrick et al., 2012ab)

191   downwards by 20 % for Br and 25 % for I. This change enables a fairer comparison of Br/Cl

192   ratios for basalt glasses obtained by the noble gas method and reported by Jambon et al.

193   (1995) and Schilling et al. (1978, 1980) (see below). However, it does not alter the

194   conclusions of the earlier studies that were based on internally consistent data sets (Kendrick

195   et al., 2012ab). A full description of the monitor re-calibration is available in the electronic

196   supplement.

197

3. Results

199   The electron microprobe and noble gas method gave similar K and Cl concentrations (Fig

200   2). The basalt glasses contain 32-1560 ppm Cl, 0.1-5.9 ppm Br and 1.6-41 ppb I, compared

201   to maxima of 3,900 ppm Cl, 14 ppm Br and 28 ppb I in the dacite glasses from the Galápagos

202   Spreading Centre (Table 1). As in previous studies, halogens have higher concentrations in

203   the more evolved samples, but each sample group has constant Br/Cl, I/Cl and K/Cl ratios

204   over a range of MgO (Table 1; Fig 3).

205   The E-MORB samples from the Mid-Atlantic Ridge (2πD43 and Famous locations) yield

206   Br/Cl of $(2.6 \pm 0.1)\times10^{-3}$ that are indistinguishable from the revised value obtained for

207   Macquarie Island E-MORB (Fig 4; Table 1; Kendrick et al., 2012b). The Atlantic E-MORB

208   have I/Cl of $(50 \pm 10)\times10^{-6}$ that are slightly less variable than those obtained for Pacific E-

209   MORB from Macquarie Island $((60 \pm 30)\times10^{-6}$; Fig 4). In contrast, K/Cl varies from values

210   of 10-12 for the Famous and Macquarie E-MORB to a distinctly higher value of 18 ± 1 for

211   2πD43 (Fig 4 and Table 1; 2σ uncertainties).

212   In comparison to the E-MORB glasses, the N-MORB glasses exhibit much greater scatter

213   in K/Cl, Br/Cl and I/Cl (Fig 4). The five glasses from the northwest part of the Lau Basin,

214   with high ^{3}He/^{4}He ratios of 12-28 Ra (Lupton et al., 2009), define a linear array in the Br/Cl

215   versus I/Cl, and Br/Cl versus K/Cl plots (Fig 4) but these parameters are not correlated with

216   ^{3}He/^{4}He (Table 1). One end-member has a composition very similar to E-MORB and the

217   second end-member has a composition similar to glasses from the Galápagos Spreading

218   Centre that are enriched in Br/Cl relative to seawater and have very low K/Cl of ~1 (Fig 4).

219

220   **4. Discussion**

221   *4.1 Inter-laboratory comparison*

222   The K and Cl concentrations of basalt glasses determined using the noble gas method

223   and electron microprobe are in good agreement with the majority of data scattering within

224   10% of the 1:1 line (Fig 2). The K and Cl concentrations determined here are also similar to

225   those reported for glasses with the same dredge numbers in previous studies, although

226　discrepancies of 10-20% exist in some cases (cf. Jambon et al., 1995; Michael and Cornell,

227　1998; Perfit et al., 1999).

228　　　　The Br/Cl ratios reported for the 19 MORB glasses in this study (Table 1), and the

229　revised values for Macquarie Island MORB (Kendrick et al., 2012b), and Society and Pitcairn

230　glasses (Kendrick et al., 2012a), overlap the ranges of Br/Cl reported by Schilling et al.

231　(1978; 1980) and Jambon et al. (1995) (Fig 5). Sample CL-DR01 yielded a Br/Cl ratio of

232　$(3.3 \pm 0.1) \times 10^{-3}$ in this study, that is approximately half the outlying value of 6.3×10^{-3}

233　reported by Jambon et al. (1995). Furthermore, sample CH98-DR11 yielded a Br/Cl ratio of

234　$(3.0 \pm 0.1) \times 10^{-3}$ in this study (Table 1) that is indistinguishable from the ratio of 3.2×10^{-3} in

235　Jambon et al. (1995), suggesting the data from these laboratories are broadly comparable at

236　the quoted levels of uncertainty (Fig 5).

237　　　　The 19 MORB glasses in this study (Table 1), and the revised values for 36 glasses

238　from Pitcairn, Society and Macquarie Island (excluding 3 outliers; Fig 4) have a mean I/Cl

239　ratio of $(60 \pm 30) \times 10^{-6}$ (2σ; Kendrick et al., 2012ab).   In comparison, the I/Cl ratios obtained

240　by combining the 14 MORB glasses analysed by Deruelle et al. (1992) and Jambon et al.

241　(1995) extend from 20×10^{-6} to a much higher value of $\sim 10^{-4}$ (Fig 5b). The highest values are

242　similar to the outlying values obtained for the Macquarie Island samples, which are attributed

243　to palagonite contamination (Fig 5b; Kendrick et al., 2012b), and iodine could have been

244　over-estimated in some of the MORB samples analysed by Dereulle et al. (1992) if the large

245　samples required for radiochemical neutron activation analysis included palagonite

246　contaminants. Very minor palagonite contamination is a potentially serious artefact in iodine

247　analyses because based on the maximum reported concentration of ~ 1 wt % organic C in

248　palagonite (Kruber et al., 2008; McLoughlin et al., 2011), and typical I/C ratios of organic

249　matter (Kennedy and Elderfield, 1987), palagonite could contain up to a ~ 1000 times more I

250　than pristine MORB glass (Table 1).

251

4.2 The Br/Cl, I/Cl and K/Cl of uncontaminated mantle melts

253   The E-MORB glasses from Macquarie Island in the SW Pacific (excluding 3 outliers;

254 Fig 4) and the samples from the Famous and popping rock locations on the Mid Atlantic

255 Ridge all have very similar Br/Cl and I/Cl ratios that define clusters rather than mixing trends

256 in Fig 4 and tight groups in Fig 5. The lack of visible mixing trends in these data implies the

257 halogens were sourced from mantle reservoirs with similar Br/Cl and I/Cl ratios (e.g. the grey

258 box in Fig 4a), and the melts did not assimilate seawater-derived halogens. The mantle origin

259 of halogens in the Macquarie Island and Famous melts is further supported by correlations

260 between the concentration of Cl and other trace elements (e.g. La, U, Ba and Nb) that have

261 low concentrations in seawater (e.g. Kamenetsky and Eggins, 2012; Kendrick et al., 2012b;

262 Michael and Cornell, 1998).

263   There are still insufficient data to define realistic ranges of Br/Cl and I/Cl in basalt

264 glasses that have not been contaminated by seawater-derived components. The E-MORB

265 glasses from Macquarie Island, Famous and Popping Rock locations all have very similar

266 Br/Cl of $(2.7 \pm 0.2) \times 10^{-3}$ (Fig 4). However, if we include ocean island basalt (OIB) glasses

267 from the Pitcairn and Society seamounts, which also appear to be free of seawater

268 contaminants (Kendrick et al., 2012a), we define typical 'mantle' values of $(2.8 \pm 0.6) \times 10^{-3}$

269 for Br/Cl and $(60 \pm 30) \times 10^{-6}$ for I/Cl (Fig 5). These data show the halogen abundance ratios

270 are surprisingly uniform with 2σ variations of only ~20 % for Br/Cl and ~50 % for I/Cl in a

271 number of MORB and OIB reservoirs. In comparison, this limited sample set has K/Cl

272 varying from 10 to 40, with a mean of 18 ± 19, demonstrating mantle Br/Cl and I/Cl are

273 much less variable than mantle K/Cl.

274   If the entire mantle has been processed to some degree, the relative degrees variation

275 in mantle Br/Cl (~20 %), I/Cl (~50 %) and K/Cl (>100 %) could reflect the geochemical

276 similarities of these elements during subduction recycling (e.g. John et al., 2011; Kendrick et

277 al., 2011; 2012a; 2013; Stroncik and Haase, 2004). Previous studies have shown Cl, Br, I and

278 K all have similar compatibilities in silicate melts with MgO of ~1-27 wt %, suggesting their

279 relative abundance ratios are fairly conservative during normal degrees of partial melting and

280 fractional crystallisation (Fig 3; Kendrick et al., 2012ab; Schilling et al., 1980).

281

282 *4.3 Assimilation of seawater-derived brines*

283   In contrast to uncontaminated MORB samples that form clusters in Figure 4, the 5

284 glasses selected from the northwest part of the Lau Basin define binary mixing arrays

285 between Br/Cl, I/Cl, K/Cl and H_2O/Cl (Figs 4 and 6; SIMS H_2O data are from Lytle et al.

286 (2012)). These mixing arrays have correlation coefficients of ~0.99, and low MSWD values

287 that demonstrate very high qualities of fit (Fig 6), and similar mixing trends are obtained for a

288 much larger data set of previously published K/Cl, F/Cl and H_2O/Cl data (Fig 7ab; Lytle et

289 al., 2012).   The mixing lines in Figures 6 and 7 are interpreted to extend from a mantle end-

290 member with K/Cl of 20 ± 10 (Fig 7a) and Br/Cl and I/Cl very similar to E-MORB (Fig 6) to

291 a second assimilated end-member that has Br/Cl, I/Cl, K/Cl and H_2O/Cl very similar to the

292 Galápagos glasses (Fig 6).

293   The high Br/Cl ratios of the assimilated components identified from the mixing trends

294 in Figs 6a and 6b are most easily explained if the melts from the Lau Basin, as well as the

295 Galápagos Spreading Centre, assimilated high salinity brines, and these data do not favour

296 alternative mechanisms of assimilating seawater-derived components (Fig 6). Assimilation of

297 alteration minerals such as amphibole (or salt) is not favoured because these minerals are

298   characterised by low Br/Cl ratios of <0.4×10^{-3} (Fontes and Matray, 1993; Holser, 1979;

299   Kendrick, 2012). As in previous studies, the H_2O/Cl ratio of the assimilated components are

300   much lower than seawater or any possible low salinity vapour-phase (Figs 6d and 7ab; Kent

301   et al., 1999ab; 2002; Michael and Schilling, 1989; Le Roux et al., 2006; Perfit et al., 1999;

302   Wanless et al., 2011). Three of the glasses have measured H_2O/Cl of 2.0-2.5 (Lytle et al.,

303   2012) and the H_2O/Cl intercepts obtained from the various regressions in Figures 6d, 7a and

304   7b are all 1.6 or lower.   These data can be reasonably interpreted to indicate a brine salinity

305   of more than 40 wt. % salts (Table 2), and a salinity of 55 ± 15 wt % salts is adopted for the

306   calculations in section 4.4.

307   Plotting H_2O, K and Cl data from previous studies in which assimilation of seawater

308   components has been investigated (Coombs et al., 2004; Le Roux et al., 2006; Kent et al.,

309   1999ab; 2002; Wanless et al., 2011), yields mixing trends that are very similar to those in

310   Figures 6d and 7a (Fig 8). These data distributions strongly suggest that brines are the

311   dominant assimilant in all the oceanic settings investigated, and furthermore that in these

312   settings the brines have a very restricted range of ultra-high salinites (e.g. 55 ± 15 wt. % salts;

313   Fig 8). The low H_2O/Cl ratios of the assimilated components are shown very clearly in our

314   three element plots that use Cl as the denominator, because the data converge on the

315   assimilant (e.g. Figs 6, 7 and 8). In contrast, variability in mantle Cl/K, H_2O/K or H_2O/Nb

316   ratios mean the uniform nature of the assimilant is masked in plots that use K or Nb as the

317   denominator (e.g. Le Roux et al., 2006; Kent et al., 1999ab; 2002; Wanless et al., 2011).

318

319   *4.4 Quantity and depth of brine assimilation*

320   The proportion of halogens assimilated by the melts included in this study can be

321   precisely quantified using the binary mixing models presented in Figures 6 and 7. The

proportion of assimilated Cl can be estimated from any X/Cl ratio that has characteristic

values in the mantle and brine (equation 1).

% assimilated Cl = [X/Cl$_{brine}$-X/Cl$_{glass}$]/[X/Cl$_{brine}$-X/Cl$_{mantle}$]×100   equation 1.

The proportion of assimilated Cl can then be converted to a Cl concentration, and because the

brine salinity is constrained as 55 ± 15 wt. % (Table 2), the concentration of H$_2$O assimilated

can also be calculated (e.g. Table 3).

Brine assimilation is quantified for five selected samples in Table 3. In each case, we

assume the brine has K/Cl of 0.02-0.2 which is a reasonable estimate for a complex solution

comprising Na$^+$, K$^+$ Ca^{++}, Mg^{++} and Fe^{++} salts (e.g. Vanko, 1988). The Br/Cl ratio of the

brine is within uncertainty of the intercepts in Figures 6a and 6b, and appears to be slightly

higher for the Lau Basin samples ((3.9 ± 0.1) ×10^{-3}) than the Galápagos Spreading Centre

((3.7 ± 0.1) ×10^{-3}) or Juan de Fuca samples ((3.6 ± 0.2) ×10^{-3}). The Lau Basin glasses show

significant spread in all chemical parameters meaning the mantle end-member can be

reasonably estimated to have K/Cl of 20 ± 10 (Fig 7a) and Br/Cl similar to E-MORB ((2.7 ±

0.2 × 10^{-3}; Figs 6a and b). In contrast, the Galapagos samples all have very low K/Cl (Fig

6d; Michael and Cornell; 1998; Perfit et al., 1999) and in this case we use two conservative

estimates for mantle K/Cl (12 ± 10 and 30 ± 20) and Br/Cl of (2.8 ± 0.6) × 10^{-3} which is

based on a wide selection of uncontaminated MORB and OIB samples (section 4.2; Table 3).

The different methods of calculation adopted in Table 3 give an indication of the

uncertainties: each method gives statistically indistinguishable results for the degree of brine

assimilation but the levels of precision vary (Table 3). Brine assimilation in the Juan de Fuca

samples is poorly resolved (Table 3), but the most contaminated samples from the Lau Basin

and all of the Galapagos Spreading Centre samples are indicated to have assimilated ~95 %

of their total Cl and 35-40 % of their total H$_2$O (Table 3). Future studies can use calculations

346 analogous to these to make reliable corrections for assimilated H_2O and Cl with quantifiable

347 uncertainty.

348   The Galápagos Spreading Centre samples with MgO of 1.6 to 6.9 wt % all have

349 indistinguishable Br/Cl (Fig 3) and I/Cl (Table 1), indicating they have assimilated similar

350 proportions of their total Cl (Fig 6). If brine assimilation occurred at an early stage of melt

351 evolution, when the melts had MgO concentrations >6.9 wt %, the maximum concentration

352 of ~12,000 ppm brine components calculated for dacite 1652-5 (Table 3) could result from

353 fractional crystallisation (Fig 3). In contrast, melts with ~7wt. % MgO from both Lau and

354 Galápagos (NLD 49-1 and 1652-10) are estimated to have assimilated 1000 to 2000 ppm of

355 brine (Table 3), which based on densities of ~1.4 g cm^{-3} for the brine and 2.9 g cm^{-3} for the

356 melt, would be equivalent to ~2-4 cm^3 of brine being assimilated per litre of melt. Note that

357 the amount of brine assimilated would be less if assimilation occurred at an even earlier stage

358 of melt evolution when the melts had >7 wt. % MgO.

359   A final constraint relevant to the interpreted assimilation mechanisms is the depth at

360 which assimilation occurs. Carbon dioxide and H_2O concentrations reported for melts from

361 the northwest part of the Lau Basin range from 2 to 240 ppm CO_2 and 0.2 to 1.3 wt % H_2O,

362 indicating CO_2 + H_2O saturation pressures of ~150 to 600 bars (Lytle et al., 2012). In

363 comparison, most of the samples were dredged from depths of only 1800 to 2400 m

364 equivalent to a pressure of <250 bars (Fig 7c; Lytle et al., 2012). These data indicate some of

365 the Lau samples with low K/Cl ratios, that assimilated up to 2000 ppm brine, were over-

366 saturated with respect to volatiles on the seafloor (Fig 7c), suggesting that brine assimilation

367 must have occurred at a higher pressure in the subsurface. If the melt assimilated the brine

368 under hydrostatic conditions, the implied depth of assimilation is more 3 km beneath the

369 seafloor (Fig 7c). Similar depths of assimilation, of up to 5 km beneath the seafloor, are

370 indicated by CO_2 and H_2O concentration data for glasses from the East Pacific Rise (le Roux

371 et al., 2006) and Hawaii (Coombs et al., 2004).

372

373 *4.5 Brine generation and assimilation mechanisms*

374   Seafloor hydrothermal vents commonly expel seawater-derived fluids with

375 temperatures of ~250-420 °C and salinities ranging from ~0.1 to 8 wt. % salts (e.g. Campbell

376 and Edmond, 1989; Coumou et al., 2009; Fontaine et al., 2007; You et al., 1994); however,

377 fluid inclusions with much higher salinities of 30-50 wt % salts are common in deeper parts

378 of the hydrothermal system (e.g. Kelley et al., 1992; 1993; Lécuyer et al., 1999; Nehlig,

379 1991; Vanko, 1988; Vanko et al. 2004). The available data suggest a portion of these brines

380 is sometimes assimilated by deep seated magmas intruding layers 2b and 3 of the crust (Figs

381 6 to 8; sections 4.3-4.4). In this section, we briefly outline how crustal brines with high Br/Cl

382 ratios (Fig 6) might be generated and why the assimilated brines have a very limited range of

383 salinity (e.g. 55 ± 15 wt. % salts; Figs 7 and 8).

384   Firstly, the average salinity of seawater-derived fluids in the oceanic crust is increased

385 by preferential incorporation of OH^-, relative to Cl^-, into hydrous alteration minerals such as

386 clays, chlorite, talc, epidote, mica, amphiboles (e.g. Ito and Anderson, 1983; Palmer, 1992;

387 Vanko, 1986). At suitably low water-rock ratios this mechanism (alone) can produce ultra-

388 saline brines and Cl-rich amphiboles with 1-4 wt. % Cl (e.g. Markl and Bucher, 1998; Vanko,

389 1986; 1988). Given the size of the amphibole anion site limits the ability of Cl^- to substitute

390 for OH^- (Volfinger et al., 1985), and because Br^- is larger than Cl^-, it is likely that amphiboles

391 have lower Br/Cl ratios than coexisting brines (e.g. Svensen et al., 2001); however, the

392 magnitude of the Br/Cl fractionation between brine and amphibole at the relevant pressure

393 and temperature conditions is unknown. Therefore it is possible that fluid-rock interactions

394 and hydration of the oceanic crust (alone) could generate fluids with the salinity (55 ± 15 wt.

395 % salts) and Br/Cl ratio of the assimilated brine (Figs 6 and 7). Alternatively, much higher

396 Br/Cl ratios ranging from $\sim 4 \times 10^{-3}$ up to 30×10^{-3} in eclogite fluid inclusions with salinities of

397 22-40 wt. % salt have previously been ascribed to this mechanism (Svensen et al., 2001).

398   Seawater-derived fluids can undergo phase separation (or hydrothermal boiling) at

399 multiple levels within the oceanic crust (Bischoff and Pitzer, 1985; Bischoff and Rosenbauer,

400 1989; Coumou et al., 2009). Adiobatic decompression produces low salinity vapours and

401 conjugate brines with up to 8 wt % salts close to the seafloor (e.g. Bischoff and Pitzer, 1985;

402 Coumou et al., 2009; Lécuyer et al., 1999). However, phase separation could occur at deeper

403 crustal levels in response to switches from lithostatic to hydrostatic pressure or heating (e.g.

404 Lécuyer et al., 1999; Vanko, 1988; Vanko et al., 2004). Brines infiltrating the cracking front

405 surrounding magma chambers in layer 3 of the crust, and brines that come into direct contact

406 with deep-seated magmas via deeply penetrating faults, will be rapidly heated to magmatic

407 temperatures (e.g. 1100-1200 °C; Bischoff and Rosenbauer, 1989). The resulting

408 superheated fluids will boil, with the vapour phase lost to the upper part of the hydrothermal

409 system and dense residual brines potentially retained in a lower layer of the crust (Fig 9;

410 Bischoff and Rosenbauer, 1989; Fontaine and Wilcock, 2006) and/or assimilated by the

411 magma (e.g. Figs 6, 7 and 8). It is possible that in this situation, the relative solubilities of

412 H_2O, Cl and Br in basaltic melts could limit the salinity (and Br/Cl) of the brine that can be

413 assimilated; e.g. the melt may become saturated with respect to H_2O but remain under-

414 saturated with respect to Cl (cf. Dixon et al., 1995; Webster et al., 1999).

415   The relative behaviour of Br and Cl during phase separation is not well constrained

416 and may vary depending on pressure and temperature conditions (e.g. Berndt and Seyfried,

417 1990; 1997; Liebscher et al., 2006; Foustoukos and Seyfried, 2007). In many cases vent

418 fluids with variable salinity preserve seawater Br/Cl ratios (Campbell and Edmond, 1989;

419   You et al., 1994), consistent with experimental data that indicate no significant fractionation

420   of Br/Cl between brines and vapours (e.g. Berndt and Seyfried, 1990; 1997). In this case, or if

421   Br is preferentially partitioned into the vapour (e.g. Foustoukos and Seyfried, 2007),

422   fractionation of Br/Cl during crustal hydration combined with phase separation could explain

423   the high Br/Cl ratios of the assimilated brines (Fig 6). However, low salinity vapours from 9-

424   10° N on the East Pacific Rise have lower than seawater Br/Cl ratios (Oosting and Von

425   Damm, 1996), which is consistent with experimental data that favour preferential partitioning

426   of Br, relative to Cl, into dense brines (Liebscher et al., 2006). Therefore it is also possible

427   that under the relevant pressure-temperature conditions, boiling off a low Br/Cl vapour phase

428   in an open system, could account for the inferred high salinity and high Br/Cl ratio of the

429   assimilated brine (Figs 6 and 7).

430   Finally, it has been suggested that further fractionation of vent fluid Br/Cl ratios could

431   result from precipitation of halite (e.g. Berndt and Seyfried, 1997; Foustoukos and Seyfried,

432   2007). This mechanism is unlikely to contribute to the Br/Cl signature of brines assimilated

433   at >400 bars (Figs 6 and 7) however, because at this pressure precipitation of halite is only

434   possible during cooling (e.g. Bodnar and Vityk, 1994). In contrast, brines at depths of >3km

435   would be heated from amphibolite facies temperatures of 500-700 °C (e.g. Vanko, 1988) to

436   magmatic temperatures of ~1100-1200 °C during assimilation (Fig 9).

437

438   *4.6 Implications for petrology and geochemistry*

439   The Br/Cl ratios of brines assimilated in the northwest part of the Lau Basin, and the

440   Galápagos Spreading Centre, are well defined by the binary mixing model in Figure 6.

441   Although a small number of samples have been analysed for Br (5 from Lau and 3 from

442   Galápagos; Fig 6), these data suggest the assimilated brines had fairly uniform Br/Cl ratios

19

443   that were slightly different in the two locations (Fig 6). The implied uniformity of the brines

444   Br/Cl (Fig 6), and the fairly uniform H_2O/Cl ratios of assimilated components elsewhere

445   (Figs 6, 7 and 8), strongly suggest that brines are efficiently segregated from OH- and Cl-

446   bearing alteration minerals before assimilation.   Assimilation of OH- and Cl-bearing

447   alteration minerals together with brines cannot explain the mixing arrays in Figures 6, 7 and

448   8, because brines mixed together with alteration minerals would have very variable Br/Cl,

449   I/Cl, K/Cl and H_2O/Cl ratios. Nonetheless the wall rocks adjacent to active magma chambers

450   at temperatures of 1100-1200 °C will have been efficiently dehydrated and are likely to have

451   very low H_2O and Cl contents. It is therefore plausible that some dehydrated wall-rock is

452   assimilated together with the brines, and this may help reconcile the halogen data that require

453   brine assimilation (and no significant assimilation of altered oceanic crust) with previously

454   reported O-isotope data that are more easily explained by wall rock assimilation (e.g. Perfit et

455   al., 1999; Wanless et al., 2011).

456   Hydrothermal brines can have ppm concentrations of elements such as Ba, Sr, Cu and

457   Pb (Coombs et al., 2004; Hardardottir et al., 2009; Schmidt et al., 2007). However, these

458   elements usually have equivalent or higher concentrations in mantle melts (e.g. Lytle et al.,

459   2012), meaning assimilation of a few hundred ppm of brine (e.g. Table 3) is unlikely to

460   perturb the mantle signatures of these elements in magmatic glasses. Similarly, it seems

461   unlikely that assimilation of a few hundred ppm of brine would greatly influence the O-

462   isotope signature of a mantle melt, unless dehydrated wall rock is assimilated with the brine

463   (above). In contrast, brine assimilation could potentially alter the mantle signatures of H-

464   isotopes, B and noble gases which all have relatively high concentrations in seawater

465   compared to the mantle (Kent et al., 1999ab). The noble gases are particularly interesting

466   because they are expected to be strongly partitioned into the vapour phase during phase

467   separation (Kennedy, 1988), and the extent to which brine assimilation influences noble gases

468   may therefore depend strongly on the role of phase separation in generating the brine (section

469   4.5).

470   Recently published data for melts from the northwest part of the Lau Basin (Hahm et

471   al., 2012; Lupton et al., 2012; Lytle et al., 2012), show that melts best preserving high

472   mantle-like H_2O/Cl ratios, appear to exhibit slightly more variation in $^3He/^4He$ than the melts

473   most influenced by brine assimilation (Fig 10a), and the melts with high mantle-like H_2O/Cl

474   ratios also preserve the highest most mantle-like $^{20}Ne/^{22}Ne$ ratios (Fig 10b). These data allow

475   the possibility that brine assimilation has influenced both the $^3He/^4He$ ratio and $^{20}Ne/^{22}Ne$

476   ratio of the Lau Basin melts. We briefly explore the feasibility of this suggestion and explore

477   its significance to demonstrate how noble gases might be combined with H_2O and halogen

478   data in future studies.

479   Brine assimilation could potentially influence the He isotope systematics of the melts

480   because even after phase separation, hydrothermal brines with negligible atmospheric helium

481   are enriched in mantle-derived (± radiogenic) helium sourced from oceanic crust by hundreds

482   of times relative to seawater helium concentrations (Kennedy, 1988). Correlations between

483   $^4He/^{40}Ar*$ and $^{36}Ar/^{40}Ar*$ in some basalt glasses have previously been interpreted as

484   indicating some helium is assimilated together with atmospheric contaminants (Fisher, 1997).

485   Brines circulated through very young oceanic crust will acquire helium with a $^3He/^4He$ ratio

486   of close to the mantle average, whereas brines circulated through older crust will be relatively

487   enriched in radiogenic ^4He. As a result, brine assimilation could have a subtle effect on the

488   $^3He/^4He$ ratios of basalt glasses, by either shifting melt $^3He/^4He$ ratios toward the crustal

489   average (e.g. Fig 10a), or perturbing the $^3He/^4He$ ratios to lower values (Graham, 2002).

490   In contrast to He, seawater has relatively high concentrations of atmospheric Ne, Ar,

491   Kr and Xe compared to the mantle (Ozima and Podosek, 2002), and seawater-derived brines

as well as altered oceanic lithosphere are dominated by atmospheric Ne, Ar, Kr and Xe isotope signatures (Kennedy, 1988; Kendrick et al., 2011; 2013; Staudacher and Allegre, 1988). If the proposed mixing trends in Fig 10b are ascribed to brine assimilation alone (and not late stage air contamination; e.g. Ballentine and Barfod, 2000), the convex shape of the trends suggests that the mantle signatures of heavy noble gases (Ne, Ar, Kr, Xe) are overprinted by brine assimilation more easily than mantle H_2O/Cl (or halogen) signatures. Furthermore, based on the Ne and Cl concentrations of the glasses investigated (Hahm et al., 2012; Lytle et al., 2012; Lupton et al., 2012), the curvature of the proposed mixing trends (Fig 10b) suggests the brines had Ne/Cl ratios broadly similar to seawater (within a factor of 5-10) and higher than the mantle. This would be possible if: atmospheric noble gases were acquired from lithological reservoirs in the sub-surface; or phase separation was a minor process in generating the brines' salinity (cf. section 4.5).

Collection of further noble gas data combined with H_2O and Cl are required to better evaluate the extent to which noble gas isotope ratios are correlated with variations in H_2O/Cl (cf. Fig 10). This is important because noble gas versus H_2O/Cl plots can be used to provide new inferences on the sources of atmospheric noble gases and address long standing uncertainties in the origin of atmospheric noble gases in pristine glasses (e.g. Patterson et al., 1990; Ballentine and Barfod, 2000). If the correlations proposed in Figure 10 are substantiated, and modern air contamination during sample preparation is shown to be a minor artefact (cf. Ballentine and Barfod, 2000), the noble gas data would provide powerful constraints on the alternative brine generation and assimilation mechanisms outlined in section 4.5.

5. Summary and Conclusions

Submarine lavas exhibit limited variation in Br/Cl and I/Cl with average and 2 standard deviation values of $[(2.8 \pm 0.6) \times 10^{-3}]$ and $[(60 \pm 30) \times 10^{-6}]$, respectively, in 43 MORB and OIB samples shown to be free of significant seawater contamination (based on correlations between Cl and other trace elements or isotopes). These ratios are invariant with respect to MgO and considered representative of the mantle sources.

Assuming the entire mantle has been processed to some degree, the relative degrees of variation in MORB and OIB Br/Cl (~20 %), I/Cl (~50 %) and K/Cl (>100 %), could reflect the behaviour of these elements during subduction. These elements do not appear to be fractionated during the degrees of partial melting and fractional crystallisation required to generate silicate melts with MgO of 1-27 wt %.

Assimilation of seawater-derived halogens can be recognised from mixing lines generated in Br/Cl, I/Cl, F/Cl, K/Cl and H_2O/Cl plots (Figs 6, 7 and 8). The H_2O/Cl and Br/Cl data do not favour the direct involvement of seawater, low salinity vapour phases or crustal alteration minerals in the assimilation process. Rather they demonstrate melts from the Lau Basin, Galápagos Spreading Centre and all other locations with anomalously Cl-rich glasses previously investigated, assimilated brines with salinities of 55 ± 15 wt. % salts (Figs 7 and 8).

The high salinity and elevated Br/Cl signature of the brines are generated by a combination of fluid-rock interaction, with preferential incorporation of $OH^- > Cl^- > Br^-$ into hydrous minerals, and phase separation. The relative importance of these processes is unknown, but open system boiling of hydrothermal fluids during, or immediately prior to, assimilation is likely to generate extremely saline brines, and the relative solubilities of Cl, Br and H_2O in basalt melts may further limit the salinity and Br/Cl ratios of the brines that can be assimilated.

540   Mixing models allow the proportion of seawater-derived H_2O and Cl introduced by

541   brine assimilation to be precisely quantified. The melts from the Lau Basin and Galápagos

542   Spreading Centre assimilated up to 35-40 % of their total H_2O and 95 % of their total Cl.

543   Similar calculations can be used to reliably correct measured H_2O and Cl abundances for

544   assimilation enabling improved estimates of mantle H_2O and Cl.

545   The widespread assimilation of seawater-derived brines, rather than seawater, implies

546   assimilation could potentially influence the helium isotope systematics of some mantle melts.

547   Plotting elemental or isotopic ratios, such as $^3He/^4He$, as a function of H_2O/Cl is an effective

548   method for assessing the extent to which the ratio is influenced by brine assimilation (e.g. Fig

549   10).

550

563

References

564

565   Bach, W. and Niedermann, S., 1998. Atmospheric noble gases in volcanic glasses from the

566   southern Lau Basin: origin from the subducting slab? *Earth and Planetary Science*

567   *Letters* **160**, 297-309.

568   Ballentine, C. J. and Barfod, D. N., 2000. The origin of air-like noble gases in MORB and

569   OIB. *Earth and Planetary Science Letters* **180**, 39-48.

570   Berndt, M. E. and Seyfried, W. E., 1990. Boron, Bromine and Other Trace-Elements as Clues

571   to the Fate of Chlorine in Midocean Ridge Vent Fluids. *Geochimica et Cosmochimica*

572   *Acta* **54**, 2235-2245.

573   Berndt, M.E., Seyfried, W.E., 1997. Calibration of Br/Cl fractionation during subcritical

574   phase separation of seawater: Possible halite at 9 to 10 degrees N East Pacific Rise.

575   Geochimica et Cosmochimica Acta, 61(14): 2849-2854.

576   Bischoff, J. L. and Rosenbauer, R. J., 1989. Salinity variations in submarine hydrothermal

577   systems by layered double-diffusive convection. *Journal of Geology* **97**, 613-623.

578   Bischoff, J.L., Pitzer, K.S., 1985. Phase relations and adiabats in boiling seafloor geothermal

579   systems. Earth and Planetary Science Letters, 75(4): 327-338.

580   Bodnar, R.J., Vityk, M.O., 1994. Interpretation of Microthermometric Data for H2O-NaCl

581   Fluid Inclusions. In: De Vivo, B., Frezzotti, M.L. (Eds.), Fluid Inclusions in Minerals;

582   Methods and Applications. Virginia Tech, Blacksburg, VA, pp. 117-130.

583   Bougault, H., Dmitriev, L., Schilling, J. G., Sobolev, A., Joron, J. L., and Needham, H. D.,

584   1988. Mantle heterogeneity from trace elements: MAR triple junction near 14°N.

585   *Earth and Planetary Science Letters* **88**, 27-36.

586   Bougault, H. and Treuil, M., 1980. Mid-Atlantic Ridge: zero-age geochemical variations

587   between Azores and 22°N. *Nature* **286**, 209-212.

588   Bryan, W.B., Thompson, G., Michael, P.J., 1979. Compositional variation in a steady-state

589   zoned magma chamber: Mid-Atlantic Ridge at 36°50′N. *Tectonophysics* **55**, 63-85.

590   Burnard, P., Graham, D., and Turner, G., 1997. Vesicle-specific noble gas analyses of

591   "popping rock"; implications for primordial noble gases in the Earth. *Science* **276**,

592   568-571.

593   Burnard, P. G., Graham, D. W., and Farley, K. A., 2002. Mechanisms of magmatic gas loss

594   along the Southeast Indian Ridge and the Amsterdam -St. Paul Plateau. *Earth and*

595   *Planetary Science Letters* **203**, 131-148.

596   Campbell, A.C., Edmond, J.M., 1989. Halide systematics of submarine hydrothermal vents.

597   *Nature*, **342** (6246): 168-170.

598   Carroll, M. R. and Holloway, J. R., 1994. Volatiles in Magmas. In: Ribbe, P. H.

599   (Ed.),Reviews in Mineralogy. Mineralogical Society of America, Washington DC.

600   Coogan, L. A., Mitchell, N. C., and O'Hara, M. J., 2003. Roof assimilation at fast spreading

601   ridges: An investigation combining geophysical, geochemical, and field evidence. *J.*

602   *Geophys. Res.-Solid Earth* **108**.

603   Coombs, M. L., Sisson, T. W., and Kimura, J. I., 2004. Ultra-high chlorine in submarine

604   Kilauea glasses: evidence for direct assimilation of brine by magma. *Earth and*

605   *Planetary Science Letters* **217**, 297-313.

606   Coumou, D., Driesner, T., Weis, P., and Heinrich, C. A., 2009. Phase separation, brine

607   formation, and salinity variation at Black Smoker hydrothermal systems. *J. Geophys.*

608   *Res.-Solid Earth* **114**.

609   Deruelle, B., Dreibus, G., and Jambon, A., 1992. Iodine abundances in oceanic basalts:

610   implications for Earth dynamics. *Earth and Planetary Science Letters* **108**, 217-227.

611   Dixon, J.E., Stolper, E.M., Holloway, J.R., 1995. An experimental study of water and carbon

612   dioxide solubilities in mid ocean ridge basaltic liquids .1. Calibration and solubility

613   models. Journal of Petrology, 36(6): 1607-1631.

614   Embley, R. W., Jonasson, I. R., Perfit, M. R., Franklin, J. M., Tivey, M. A., Malahoff, A.,

615   Smith, M. F., and Francis, T. J. G., 1988. Submersible Investigation of an Extinct

616   Hydrothermal System on the Galapagos Ridge - Sulfide Mounds, Stockwork Zone,

617   and Differentiated Lavas. *Canadian Mineralogist* **26**, 517-539.

618   Filiberto, J. and Treiman, A. H., 2009. The effect of chlorine on the liquidus of basalt: First

619   results and implications for basalt genesis on Mars and Earth. *Chemical Geology* **263**,

620   60-68.

621   Fisher, D. E., 1997. Helium, argon, and xenon in crushed and melted MORB. *Geochimica et*

622   *Cosmochimica Acta* **61**, 3003-3012.

623   Fontaine, F. J. and Wilcock, W. S. D., 2006. Dynamics and storage of brine in mid-ocean

624   ridge hydrothermal systems. *J. Geophys. Res.-Solid Earth* **111**.

625   Fontaine, F.J., Wilcock, W.S.D., Butterfield, D.A., 2007. Physical controls on the salinity of

626   mid-ocean ridge hydrothermal vent fluids. *Earth and Planetary Science Letters*,

627   **257**(1-2): 132-145.

628   Fontes, J. C. and Matray, J. M., 1993. Geochemistry and origin of formation brines from the

629   Paris Basin, France 1. Brines associated with Triassic salts. *Chemical Geology* **109**,

630   149-175.

631   Foustoukos, D.I., Seyfried, W.E., 2007. Trace element partitioning between vapor, brine and

632   halite under extreme phase separation conditions. *Geochimica et Cosmochimica Acta,*

633   **71**(8): 2056-2071.

634   Graham, D. W., 2002. Noble Gas Isotope Geochemistry of Mid-Ocean Ridge and Ocean

635   Island Basalts: Characterisation of Mantle Source Reservoirs. In: Porcelli, D.,

636   Ballentine, C. J., and Wieler, R. Eds.), Noble Gases in Geochemistry and

637   Cosmochemistry.

638 Hahm, D., Hilton, D. R., Castillo, P. R., Hawkins, J. W., Hanan, B. B., and Hauri, E. H.,

639   2012. An overview of the volatile systematics of the Lau Basin – Resolving the

640   effects of source variation, magmatic degassing and crustal contamination.

641   *Geochimica et Cosmochimica Acta* **85**, 88-113.

642 Hammerli, J., Rusk, B., Spandler, C., Emsbo, P., and Oliver, N. H. S., 2013. In situ

643   quantification of Br and Cl in minerals and fluid inclusions by LA-ICP-MS: A

644   powerful tool to identify fluid sources. *Chemical Geology* **337–338**, 75-87.

645 Hardardottir, V., Brown, K. L., Fridriksson, T., Hedenquist, J. W., Hannington, M. D., and

646   Thorhallsson, S., 2009. Metals in deep liquid of the Reykjanes geothermal system,

647   southwest Iceland: Implications for the composition of seafloor black smoker fluids.

648   *Geology* **37**, 1103-1106.

649 Hekinian, R., Fevrier, M., Avedik, F., Cambon, P., Charlou, J. L., Needham, H. D., Raillard,

650   J., Boulegue, J., Merlivat, L., Moinet, A., Manganini, S., and Lange, J., 1983. East

651   Pacific Rise Near 13-Degrees-N - Geology of New Hydrothermal Fields. *Science* **219**,

652   1321-1324.

653 Hilton, D. R. and Porcelli, D., 2003. Noble Gases as Mantle Tracers. In: Carlson, R. L. (Ed.),

654   The Mantle and Core - Treatise of Geochemistry. Elsevier, Oxford.

655 Hofmann, A. W., 2003. Sampling Mantle Heterogeneity through Oceanic Basalts: Isotopes

656   and Trace Elements. In: Carlson, R. L. (Ed.), Treatise of Geochemistry Volume 2:

657   The Core and Mantle. Elsevier Ltd.

658 Holser, W. T., 1979. Trace elements and isotopes in evaporites. In: Burns, R. G. (Ed.),

659   Marine minerals: Mineralogical Society of America Short Course Notes.

660   Ito, E., Anderson, A.T., Jr., 1983. Submarine metamorphism of gabbros from the Mid-

661   Cayman Rise: Petrographic and mineralogic constraints on hydrothermal processes at

662   slow-spreading ridges. Contributions to Mineralogy and Petrology, 82(4): 371-388.

663   Ito, E., Harris, D. M., and Anderson, A. T., 1983. Alteration of Oceanic-Crust and Geologic

664   Cycling of Chlorine and Water. *Geochimica et Cosmochimica Acta* **47**, 1613-1624.

665   Jambon, A., Deruelle, B., Dreibus, G., and Pineau, F., 1995. Chlorine and bromine abundance

666   in MORB: The contrasting behaviour of the Mid-Atlantic Ridge and East Pacific Rise

667   and implications for chlorine geodynamic cycle. *Chemical Geology* **126**, 101-117.

668   John, T., Scambelluri, M., Frische, M., Barnes, J.D., Bach, W., 2011. Dehydration of

669   subducting serpentinite: Implications for halogen mobility in subduction zones and

670   the deep halogen cycle. Earth and Planetary Science Letters, 308(1-2): 65-76.

671   Kamenetsky, V. S. and Eggins, S. M., 2012. Systematics of metals, metalloids, and volatiles

672   in MORB melts: Effects of partial melting, crystal fractionation and degassing (a case

673   study of Macquarie Island glasses). *Chemical Geology* **302**, 76-86.

674   Kelley, D. S., Gillis, K. M., and Thompson, G., 1993. Fluid evolution in submarine magma-

675   hydrothermal systems at the Mid-Atlantic Ridge. *J. Geophys. Res.-Solid Earth* **98**,

676   19579-19596.

677   Kelley, D. S., Robinson, P. T., and Malpas, J. G., 1992. Processes of brine generation and

678   circulation in the oceanic-crust – Fluid inclusion evidence from the Troodos

679   Ophiolite, Cyprus. *J. Geophys. Res.-Solid Earth* **97**, 9307-9322.

680   Kendrick, M. A., 2012. High precision Cl, Br and I determination in mineral standards using

681   the noble gas method. *Chemical Geology* **292-293**, 116-126.

682   Kendrick, M. A., Honda, M., Pettke, T., Scambelluri, M., Phillips, D., and Giuliani, A., 2013.

683   Subduction zone fluxes of halogens and noble gases in seafloor and forearc

684   serpentinites. *Earth and Planetary Science Letters* **365**, 86-96.

685   Kendrick, M. A., Kamenetsky, V. S., Phillips, D., and Honda, M., 2012a. Halogen (Cl, Br, I)

686   systematics of mid-ocean ridge basalts: a Macquarie Island case study. *Geochimica et*

687   *Cosmochimica Acta* **81**, 82-93.

688   Kendrick, M. A., Scambelluri, M., Honda, M., and Phillips, D., 2011. High abundances of

689   noble gas and chlorine delivered to the mantle by serpentinite subduction. *Nat.*

690   *Geosci.* **4**, 807-812.

691   Kendrick, M. A., Woodhead, J. D., and Kamenetsky, V. S., 2012b. Tracking halogens

692   through the subduction cycle. *Geology* **40**, 1075-1078.

693   Kennedy, B. M., 1988. Noble gases in vent water from the Juan de Fuca Ridge. *Geochimica*

694   *et Cosmochimica Acta* **52**, 1929-1935.

695   Kennedy, H. A. and Elderfield, H., 1987. Iodine diagenesis in pelagic deep sea sediments.

696   *Geochemica et Cosmochemica Acta* **51**, 2489-2504.

697   Kent, A. J. R., Clague, D. A., Honda, M., Stolper, E. M., Hutcheon, I. D., and Norman, M.

698   D., 1999a. Widespread assimilation of a seawater-derived component at Loihi

699   Seamount, Hawaii. *Geochimica et Cosmochimica Acta* **63**, 2749-2761.

700   Kent, A. J. R., Norman, M. D., Hutcheon, I. D., and Stolper, E. M., 1999b. Assimilation of

701   seawater-derived components in an oceanic volcano: evidence from matrix glasses

702   and glass inclusions from Loihi seamount, Hawaii. *Chemical Geology* **156**, 299-319.

703   Kent, A. J. R., Peate, D. W., Newman, S., Stolper, E. M., and Pearce, J. A., 2002. Chlorine in

704   submarine glasses from the Lau Basin: seawater contamination and constraints on the

705   composition of slab-derived fluids. *Earth and Planetary Science Letters* **202**, 361-

706   377.

707   Kruber, C., Thorseth, I. H., and Pedersen, R. B., 2008. Seafloor alteration of basaltic glass:

708   Textures, geochemistry, and endolithic microorganisms. *Geochem. Geophys. Geosyst.*

709   **9**.

710   Langmuir, C. H., Bender, J. F., Bence, A. E., and Hanson, G. N., 1977. Petrogenesis of

711   Basalts from the FAMOUS Area: Mid-Atlantic Ridge. *Earth and Planetary Science*

712   *Letters* **36**, 133-156.

713   Langmuir, C. H., Vocke Jr, R. D., Hanson, G. N., and Hart, S. R., 1978. A general mixing

714   equation with applications to Icelandic basalts. *Earth and Planetary Science Letters*

715   **37**, 380-392.

716   le Roux, P. J., Shirey, S. B., Hauri, E. H., Perfit, M. R., and Bender, J. F., 2006. The effects

717   of variable sources, processes and contaminants on the composition of northern EPR

718   MORB (8-10 degrees N and 12-14 degrees N): Evidence from volatiles (H_2O, CO_2, S)

719   and halogens (F, Cl). *Earth and Planetary Science Letters* **251**, 209-231.

720   Lécuyer, C. et al., 1999. Phase separation and fluid mixing in subseafloor back arc

721   hydrothermal systems: A microthermometric and oxygen isotope study of fluid

722   inclusions in the barite-sulfide chimneys of the Lau Basin. Journal of Geophysical

723   Research: Solid Earth, 104(B8): 17911-17927.

724   Liebscher, A., Luders, V., Heinrich, W., and Schettler, G., 2006. Br/Cl signature of

725   hydrothermal fluids: liquid-vapour fractionation of bromine revisited. *Geofluids* **6**,

726   113-121.

727   Litasov, K. D., Ohtani, E., and Sano, A., 2006. Influence of Water on Major Phase

728   Transitions in the Earth's Mantle. In: Jacobsen, S. B. and Lee, S. v. d. Eds.), Earth's

729   Deep Water Cycle. American Geophysical Union.

730   Ludwig, K. R., 2009. User's manual for Isoplot 3.7. Berkeley Geochronology Center Special

731   Publication No. 4.

732   Lupton, J. E., Arculus, R. J., Evans, L. J., and Graham, D. W., 2012. Mantle hotspot neon in

733   basalts from the Northwest Lau Back-arc Basin. *Geophysical Research Letters* **39**.

734   Lupton, J. E., Arculus, R. J., Greene, R. R., Evans, L. J., and Goddard, C. I., 2009. Helium

735   isotope variations in seafloor basalts from the Northwest Lau Backarc Basin:

736   Mapping the influence of the Samoan hotspot. *Geophysical Research Letters* **36**.

737   Lytle, M. L., Kelley, K. A., Hauri, E. H., Gill, J. B., Papia, D., and Arculus, R. J., 2012.

738   Tracing mantle sources and Samoan influence in the northwestern Lau back-arc basin.

739   *Geochemistry, Geophysics, Geosystems* **13**, n/a-n/a.

740   Markl, G., Bucher, K., 1998. Composition of fluids in the lower crust inferred from

741   metamorphic salt in lower crustal rocks. Nature, 391(6669): 781-783.

742   Marty, B. and Humbert, F., 1997. Nitrogen and argon isotopes in oceanic basalts. *Earth and*

743   *Planetary Science Letters* **152**, 101-112.

744   Marty, B. and Zimmermann, L., 1999. Volatiles (He, C, N, Ar) in mid-ocean ridge basalts:

745   assesment of shallow-level fractionation and characterization of source composition.

746   *Geochimica et Cosmochimica Acta* **63**, 3619-3633.

747   McLoughlin, N., Wacey, D., Kruber, C., Kilburn, M. R., Thorseth, I. H., and Pedersen, R. B.,

748   2011. A combined TEM and NanoSIMS study of endolithic microfossils in altered

749   seafloor basalt. *Chemical Geology* **289**, 154-162.

750   Michael, P. J. and Cornell, W. C., 1998. Influence of spreading rate and magma supply on

751   crystallization and assimilation beneath mid-ocean ridges: Evidence from chlorine

752   and major element chemistry of mid-ocean ridge basalts. *J. Geophys. Res.-Solid Earth*

753   **103**, 18325-18356.

754   Michael, P. J. and Schilling, J.-G., 1989. Chlorine in mid-ocean ridge magmas: Evidence for

755   assimilation of seawater-influenced components. *Geochimica et Cosmochimica Acta*

756   **53**, 3131-3143.

757   Moreira, M., Kunz, J., and Allegre, C., 1998. Rare gas systematics in popping rock: Isotopic

758   and elemental compositions in the upper mantle. Science **279**, 1178-1181.

759 Mukhopadhyay, S., 2012. Early differentiation and volatile accretion recorded in deep-mantle
760   neon and xenon. *Nature* **486**, 101-104.

761 Nehlig, P., 1991. Salinity of oceanic hydrothermal fluids: a fluid inclusion study. *Earth and*
762   *Planetary Science Letters* **102**, 310-325.

763 Newman, S., Lowenstern, J.B., 2002. VOLATILECALC: a silicate melt-H2O-CO2 solution
764   model written in Visual Basic for excel. Computers & Geosciences, 28(5): 597-604.

765 Nishio, Y., Sasaki, S., Gamo, T., Hiyagon, H., and Sano, Y., 1998. Carbon and helium
766   isotope systematics of North Fiji Basin basalt glasses: carbon geochemical cycle in
767   the subduction zone. *Earth and Planetary Science Letters* **154**, 127-138.

768 Oosting, S.E., Von Damm, K.L., 1996. Bromide/chloride fractionation in seafloor
769   hydrothermal fluids from 9–10°N East Pacific Rise. Earth and Planetary Science
770   Letters, 144(1–2): 133-145.

771 Ozima, M., Podosek, F.A., 2002. Noble Gas Geochemistry. Cambridge University Press.

772 Palmer, M. R., 1992. Controls over the chloride concentration of submarine hydrothermal
773   vent fluids: evidence from Sr/Ca and $^{87}Sr/^{86}Sr$ ratios. *Earth and Planetary Science*
774   *Letters* **109**, 37-46.

775 Patterson, D. B., Honda, M., and McDougall, I., 1990. Atmospheric Contamination: A
776   Possible Sorce for Heavy Noble Gases in Basalts from Loihi Seamount, Hawaii.
777   *Geophysical Research Letters* **17**, 705-708.

778 Perfit, M. R., Cann, J. R., Fornari, D. J., Engels, J., Smith, D. K., Ian Ridley, W., and
779   Edwards, M. H., 2003. Interaction of sea water and lava during submarine eruptions at
780   mid-ocean ridges. *Nature* **426**, 62-65.

781 Perfit, M.R., Ridley, W.I., Jonasson, I.R., 1999. Geologic, petrologic and geochemical
782   relationships between magmatism and massive sulfide mineralization along the
783   eastern Galapagos Spreading Center. In: C.T., B., Hannington, M.D. (Editors),

784 Volcanic Associated Massive Sulfide Deposits: Processes and Examples in Modern

785 and Ancient Settings. Reviews in Economic Geology. The Society of Economic

786 Geologists, pp. 75-99.

787 Saal, A. E., Hauri, E. H., Langmuir, C. H., and Perfit, M. R., 2002. Vapour undersaturation in

788 primitive mid-ocean-ridge basalt and the volatile content of Earth's upper mantle.

789 *Nature* **419**, 451-455.

790 Sano, T., Miyoshi, M., Ingle, S., Banerjee, N.R., Ishimoto, M., Fukuoka, T., 2008. Boron and

791 chlorine contents of upper oceanic crust: Basement samples from IODP Hole 1256D.

792 *Geochemistry, Geophysics, Geosystems* **9**, Q12O15.

793 Sarda, P., 2004. Surface noble gas recycling to the terrestrial mantle. *Earth and Planetary*

794 *Science Letters* **228**, 49-63.

795 Scambelluri, M., Piccardo, G. B., Philippot, P., Robbiano, A., and Negretti, L., 1997. High

796 salinity fluid inclusions fromed from recycled seawater in deeply subducted alpine

797 serpentinite. *Earth and Planetary Science Letters* **148**, 485-499.

798 Schilling, J. C., Unni, C. K., and Bender, M. L., 1978. Origin of Chlorine and Bromine in the

799 oceans. *Nature* **273**, 631-636.

800 Schilling, J. G., Bergeron, M. B., and Evans, R., 1980. Halogens in the mantle beneath the

801 North Atlantic. *Philos. Trans. R. Soc. Lond. Ser. A-Math. Phys. Eng. Sci.* **297**, 147-

802 178.

803 Schmidt, K., Koschinsky, A., Garbe-Schönberg, D., de Carvalho, L. M., and Seifert, R.,

804 2007. Geochemistry of hydrothermal fluids from the ultramafic-hosted Logatchev

805 hydrothermal field, 15°N on the Mid-Atlantic Ridge: Temporal and spatial

806 investigation. *Chemical Geology* **242**, 1-21.

807 Seyfried, W. E., Jr., Seewald, J. S., Berndt, M. E., Ding, K., and Foustoukos, D. I., 2003.

808 Chemistry of hydrothermal vent fluids from the Main Endeavour Field, northern Juan

809   de Fuca Ridge: Geochemical controls in the aftermath of June 1999 seismic events. *J.*

810   *Geophys. Res.* **108**, 2429.

811   Smith, M. C., Perfit, M. R., and Jonasson, I. R., 1994. Petrology and Geochemistry of Basalts

812   from the Southern Juan De Fuca Ridge - Controls on the Spatial and Temporal

813   Evolution of Mid-Ocean Ridge Basalt. *J. Geophys. Res.-Solid Earth* **99**, 4787-4812.

814   Soule, S. A., Fornari, D. J., Perfit, M. R., Ridley, W. I., Reed, M. H., and Cann, J. R., 2006.

815   Incorporation of seawater into mid-ocean ridge lava flows during emplacement. *Earth*

816   *and Planetary Science Letters* **252**, 289-307.

817   Staudacher, T. and Allègre, C. J., 1988. Recycling of oceanic crust and sediments: the noble

818   gas subduction barrier. *Earth and Planetary Science Letters* **89**, 173-183.

819   Staudacher, T., Sarda, P., Richardson, S. H., Allegre, C. J., Sagna, I., and Dmitriev, L. V.,

820   1989. Noble-Gases in Basalt Glasses from a Mid-Atlantic Ridge Topographic High at

821   14 degrees-N - Geodynamic Consequences. *Earth and Planetary Science Letters* **96**,

822   119-133.

823   Straub, S.M., Layne, G.D., 2003. The systematics of chlorine, fluorine, and water in Izu arc

824   front volcanic rocks: Implications for volatile recycling in subduction zones.

825   Geochimica Et Cosmochimica Acta, 67(21): 4179-4203.

826   Stroncik, N.A., Haase, K.M., 2004. Chlorine in oceanic intraplate basalts: Constraints on

827   mantle sources and recycling processes. Geology, 32(11): 945-948.

828   Svensen, H., Banks, D. A., and Austreim, H., 2001. Halogen contents of eclogite facies fluid

829   inclusions and minerals: Caledonides, western Norway. *Journal of Metamorphic*

830   *Geology* **19**, 165-178.

831   Trieloff, M., Falter, M., and Jessberger, E. K., 2003. The distribution of mantle and

832   atmospheric argon in oceanic basalt glasses. *Geochimica Et Cosmochimica Acta* **67**,

833   1229-1245.

834 Unni, C. K. and Schilling, J. G., 1977. Determination of Bromine in Silicate Rocks by

835   epithermal Neutron-Activation Analysis. Analytical Chemistry **49**, 1998-2000.

836 Unni, C. K. and Schilling, J. G., 1978. Cl and Br Degassing by Volcanism Along Reykjanes

837   Ridge and Iceland. *Nature* **272**, 19-23.

838 Vanko, D. A., 1986. High-chlorine amphiboles from oceanic rocks: product of highly-saline

839   hydrothermal fluids? *Am. Miner.* **71**, 51-59.

840 Vanko, D.A., 1988. Temperature, pressure, and composition of hydrothermal fluids, with

841   their bearing on the magnitude of tectonic uplift at mid-ocean ridges, inferred from

842   fluid inclusions in oceanic layer 3 rocks. Journal of Geophysical Research: Solid

843   Earth, 93(B5): 4595-4611.

844 Vanko, D.A., Bach, W., Roberts, S., Yeats, C.J., Scott, S.D., 2004. Fluid inclusion evidence

845   for subsurface phase separation and variable fluid mixing regimes beneath the deep-

846   sea PACMANUS hydrothermal field, Manus Basin back arc rift, Papua New Guinea.

847   Journal of Geophysical Research-Solid Earth, 109(B3).

848 Volfinger, M., Robert, J.L., Vielzeuf, D., Neiva, A.M.R., 1985. Structural control of the

849   chlorine content of OH-bearing silicates (micas and amphiboles). Geochimica et

850   Cosmochimica Acta, 49(1): 37-48.

851 Wanless, V. D., Perfit, M. R., Ridley, W. I., and Klein, E., 2010. Dacite Petrogenesis on Mid-

852   Ocean Ridges: Evidence for Oceanic Crustal Melting and Assimilation. *J. Petrol*. **51**,

853   2377-2410.

854 Wanless, V.D. et al., 2011. Volatile abundances and oxygen isotopes in basaltic to dacitic

855   lavas on mid-ocean ridges: The role of assimilation at spreading centers. Chemical

856   Geology, 287(1–2): 54-65.

857   Webster, J.D., Kinzler, R.J., Mathez, E.A., 1999. Chloride and water solubility in basalt and

858   andesite melts and implications for magmatic degassing. Geochimica Et

859   Cosmochimica Acta, 63(5): 729-738.

860   You, C.F. et al., 1994. Boron and halide systematics in submarine hydrothermal systems:

861   Effects of phase separation and sedimentary contributions. Earth and Planetary

862   Science Letters, 123(1-3): 227-238.

863

Table 1. Basalt Glass total fusion halogen data (2σ analytical uncertainty)

Sample name	MgO Wt.%	(La/Sm)$_N$	^{3}He/^{4}He R/Ra	Mass (mg)	Cl ppm	Br ppb	I ppb	K wt.%	Br/Cl (wt.) ×10^{-3}	I/Cl (wt.) ×10^{-6}	K/Cl (wt.)
Mid-Atlantic Ridge Famous area (36° 50'N)											
Alv 529-4	*9.1*	*1.0*		19.4	111	300	4.5	0.11	2.69 ± 0.08	40 ± 6	10.3 ± 0.7
Alv 523-1	*8.5*	1.5		9.3	135	350	7.2	0.17	2.59 ± 0.08	53 ± 20	12.3 ± 0.8
Alv 526-5	*7.9*	1.4		23.3	167	446	8.2	0.18	2.7 ± 0.1	49 ± 2	10.7 ± 0.7
Alv 525-5-2	*9.9*	1.2		8.0	81	215	3.2	0.08	2.65 ± 0.09	39 ± 9	10.2 ± 0.7
Alv 527-1-1	*9.7*	1.0		9.3	39	95	1.6	0.05	2.46 ± 0.09	40 ± 15	11.6 ± 0.8
Mid-Atlantic Ridge MAPCO (30-32°N)											
CH98-DR08g3	6.7	1.4		30.0	630	1,900	20	0.10	3.0 ± 0.1	32 ± 2	1.6 ± 0.1
CH98-DR11	8.4	0.5	*8.2*	27.2	32	97	2.0	0.03	3.01 ± 0.07	63 ± 3	10.0 ± 0.8
Mid-Atlantic Ridge popping rock (13° 50'N)											
2πD43-1	7.7	1.9	*8.2-8.5*	14.9	282	730	14	0.52	2.6 ± 0.1	49 ± 3	18 ± 1
2πD43-2	7.7	1.9	*8.2-8.5*	11.6	285	740	15	0.52	2.6 ± 0.1	52 ± 4	18 ± 1
2πD43-3	7.7	1.9	*8.2-8.5*	14.7	265	689	12	0.48	2.60 ± 0.08	44 ± 2	18 ± 1
2πD43-4	7.7	1.9	*8.2-8.5*	7.2	290	757	15	0.52	2.61 ± 0.06	53 ± 4	18 ± 1
Juan de Fuca (45 - 46°N)											
Alv 2262-8	7.7	0.7		15.3	86	256	2.5	0.10	3.0 ± 0.1	29 ± 4	11.9 ± 0.8
Alv 2269-2	7.1	0.7		14.8	154	488	2.9	0.12	3.2 ± 0.1	19 ± 1	7.6 ± 0.5
Galápogos spreading centre (0-1°N)											
Alv 1652-3	1.5	0.7		13.2	3,790	13,600	27	0.31	3.6 ± 0.1	7.0 ± 0.4	0.8 ± 0.1
Alv 1652-10	6.9	0.5		12.0	340	1,230	2.4	0.05	3.6 ± 0.1	7.2 ± 2.7	1.6 ± 0.1
Alv 1652-5	1.6	0.7		19.0	3,870	13,900	28	0.31	3.6 ± 0.1	7.4 ± 0.4	0.81 ± 0.05
East Pacific Rise Clipperton (12° 50'N)											
CL-DR01	7.9	0.8	*8.1 ± 0.2*	28.9	92	309	3.7	0.10	3.34 ± 0.09	40 ± 2	10.9 ± 0.8
North west Lau Basin (14-16 S°)											
NLD 20-1	*9.1*	*1.2*	*18.6*	24.0	163	549	4.2	0.11	3.36 ± 0.09	26 ± 2	6.6 ± 0.4
NLD 39-1			*12.0*	18.1	1,560	5,900	15	0.23	3.79 ± 0.07	9.4 ± 0.4	1.5 ± 0.1
NLD 49-1	*7.0*	*0.5*	*20.8*	16.5	635	2,420	5.1	0.06	3.81 ± 0.07	8.0 ± 1.0	0.9 ± 0.1
NLD 13-1	*8.6*	*0.7*	*28.1*	14.0	67	210	2.4	0.07	3.12 ± 0.07	36 ± 3	10.2 ± 0.7
NLD 48-1	*8.4*	*0.4*	*15.9*	15.9	340	1,290	4.0	0.03	3.78 ± 0.09	12 ± 1	1.0 ± 0.1
Mac. Is. E-MORB	*5.9-8.8*	*0.9-4.9*	*7.1-8.3*						2.67 ± 0.05	65 ± 7	11.1 ± 0.5
Seawater					19,400	65,877	58	0.038	3.5	3.1	0.02

Additional major and trace element data are available in the electronic supplement. Italicised values for MgO, La/Sm and ^{3}He/^{4}He are published values (Langmuir et al., 1977; Lupton et al., 2009; Lytle et al., 2012; Marty and Zimmermann, 1999; Moreira et al., 1998; Nishio et al., 1998). Macquarie Island data are revised according the revised Br/Cl and I/Cl ratios of the scapolite standards (Fig 1; Kendrick et al., 2013). Note that ^{3}He/^{4}He ratios are reported as R/Ra where Ra is the atmospheric ^{3}He/^{4}He ratio of 1.39×10^{-6}. E-MORB form a continuum with N-MORB are defined here as having primitive mantle normalised La/Sm [(La/Sm)$_N$] of > 1 (Hofmann, 2003).

Table 2. Estimated brine salinity

H$_2$O/Cl	Wt. % Salts[1]	Wt.% NaCl eq.	comments
Northwest part of the Lau Basin			
<2.5	>42	>37	Min. meas. H$_2$O/Cl
<2.0	>48	>42	(Lytle et al., 2012)
0.7 ± 0.5	60-90	55-90	Fig 6d
$0.6^{+1.6}_{-1.3}$	>45	>40	Fig 7a; NWL data
$1.6^{+1.4}_{-1.0}$	38-75	33-70	Fig 7a; all data
$-0.0^{+0.8}_{-1.0}$	>70	>64	Fig 7b; NWL data
$-1.0^{+0.8}_{-0.8}$			Fig 7b; all data

1 – wt. % salts calculated assuming the composition of seawater salt with a Cl weight fraction of 0.55.

Table 3. Quantification of brine assimilation in selected samples (2σ uncertainties)

Sample	Measured Cl ppm	Measured H_2O wt. %[2]	Assim. Cl %	Calculated Assim Cl ppm	Calculated Assim. brine ppm	Assim. H_2O %	Basis of calculation[1]
Lau Basin							
NLD 49-1	635	0.25	96 ± 2	610 ± 10	2000 ± 600	36 ± 8	K-1
			92 ± 12	580 ± 80	1900 ± 600	35 ± 15	Br-1
NLD 13-1	67	0.25	49 ± 26	33 ± 17	110 ± 60	2 ± 1	K-1
			33 ± 17	22 ± 11	70 ± 40	1.7 ± 0.4	Br-1
Galápagos Spreading Centre							
Alv 1652-10	340	0.26	87 ± 11	300 ± 40	980 ± 290	17 ± 4	K-2
			95 ± 3	320 ± 10	1100 ± 300	18 ± 4	K-3
			89 ± 17	300 ± 60	1000 ± 300	18 ± 8	Br-2
Alv 1652-5	3,870	1.38	94 ± 5	3600 ± 200	12000 ± 3000	39 ± 8	K-2
			89 ± 17	3400 ± 700	11000 ± 4000	37 ± 16	Br-2
Juan de Fuca							
Alv 2269-2	154		40 ± 50	60 ± 80	190 ± 280		K-2
			50 ± 50	80 ± 80	260 ± 260		Br-2

1- Sample K/Cl and Br/Cl are given in Table 1. All brines are assumed to have K/Cl of 0.1 ± 0.09 and 55 ± 15 wt. % salts (comprising 0.55 Cl by mass). Brine Br/Cl (estimated from Fig 6a) are $(3.9 ± 0.1)×10^{-3}$ for Lau; $(3.7 ± 0.1)×10^{-3}$ for Galápagos; and $(3.6 ± 0.2)×10^{-3}$ for Juan de Fuca. Mantle K/Cl values are: 20 ± 10 (K-1); 12 ± 10 (K-2); or 30 ± 20 (K-3). Mantle Br/Cl values are: $(2.7 ± 0.2)×10^{-3}$ (Br-1) or $(2.8 ± 0.6)×10^{-3}$ (Br-2).

2- Water concentrations from Lytle et al. (2012) and Perfit et al. (1999).
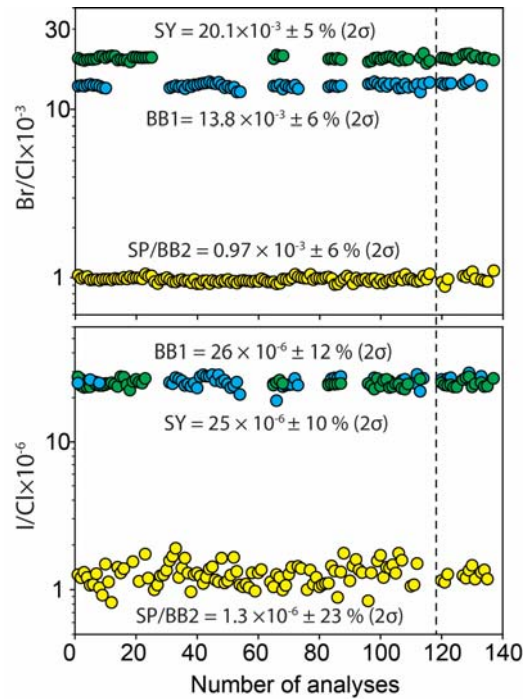
Fig 1 (Kendrick et al., 2013)

Fig 1. Scapolite standards used to monitor the production of $^{38}Ar_{Cl}$, $^{80}Kr_{Br}$ and $^{128}Xe_I$ in 7 irradiations have good reproducibility (Kendrick, 2012). The absolute Br/Cl and I/Cl ratios recommended for the monitors have been revised using a combination of techniques described in the supplementary information (Kendrick et al., 2013). Analyses 1-119 were undertaken by laser microanalysis (Kendrick, 2012), but the more recent analyses have been undertaken by fusing scapolites in a resistance furnace, enabling improved measurement of iodine in samples SP/BB2 (supplementary information).

Fig 2 (Kendrick et al., 2013)
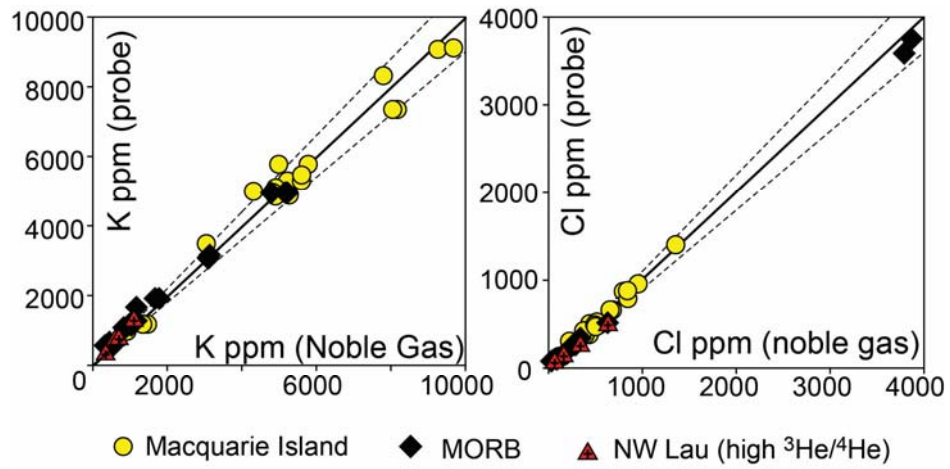
Fig 2. K and Cl concentrations of glasses determined from irradiation produced $^{39}Ar_K$ and $^{38}Ar_{Cl}$ using the noble gas method and electron microprobe data show good agreement. The 1:1 reference line and a 10% envelope are shown for reference.

Fig 3 (Kendrick et al., 2013)
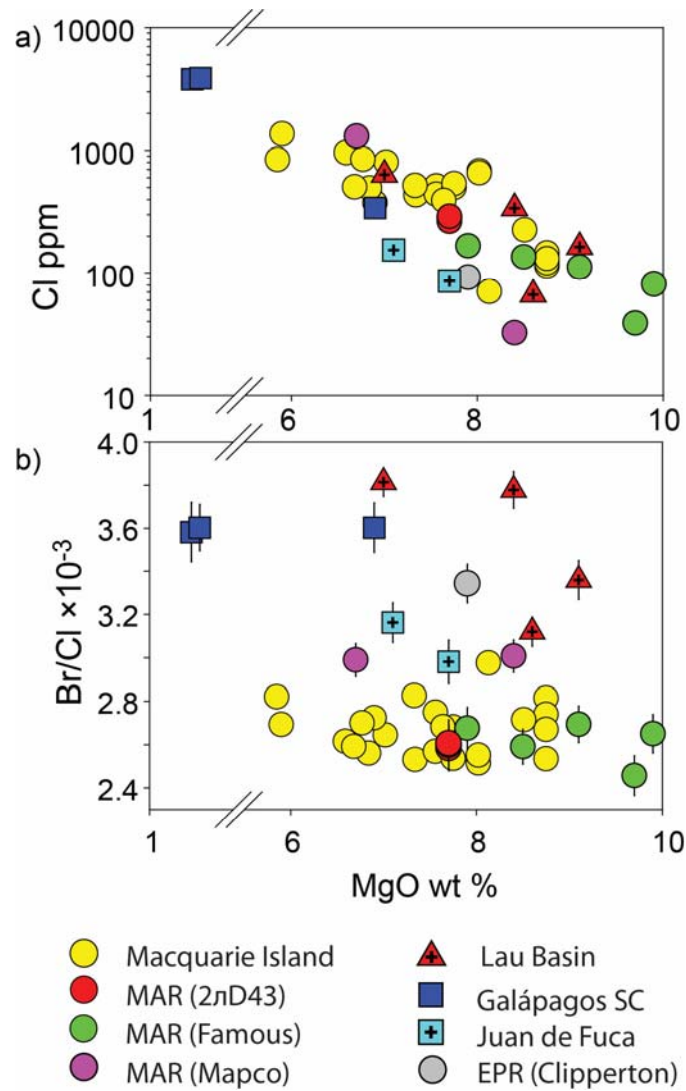
Fig 3. The Cl concentration and Br/Cl of magmatic glasses versus MgO (note the break in scale on the x-axis). The most evolved glasses have the highest Cl concentrations but the constancy of Br/Cl within any sample group over a range of MgO indicates Br/Cl is not fractionated as a function of partial melting or fractional crytsalisation (see also (Kendrick et al., 2012a).

Fig 4 (Kendrick et al., 2013)
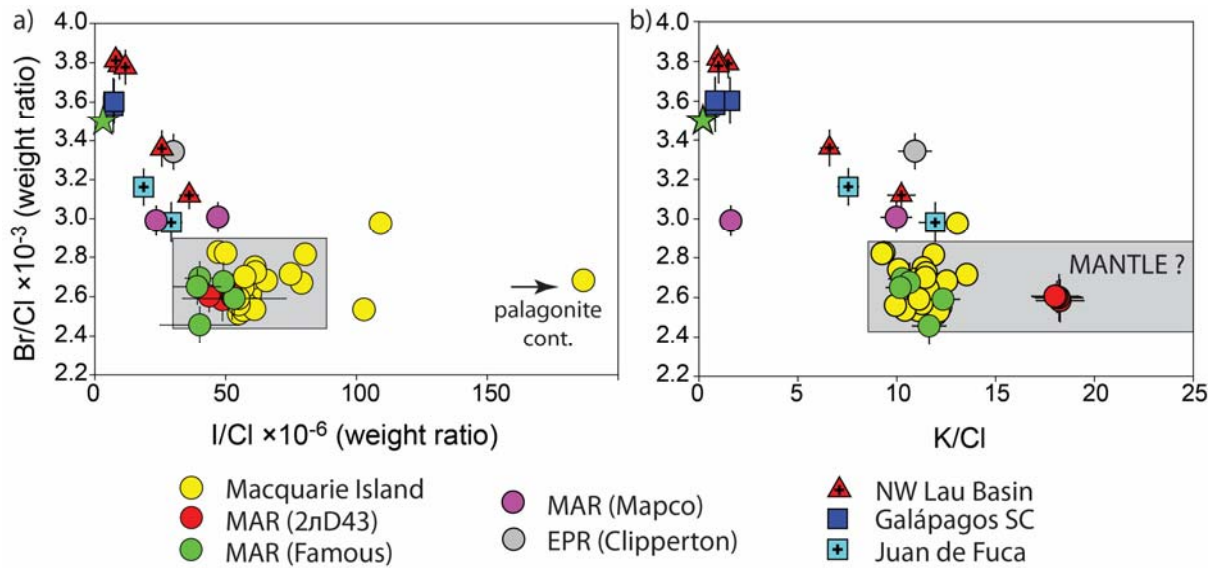
Fig 4. Halogen and K three element plots for the samples in this study: a) Br/Cl versus I/Cl, and b) Br/Cl versus K/Cl. The composition of seawater is shown as a star in both panels. The grey box in 'a' highlights the mean and 2 standard deviation values of Br/Cl and I/Cl ratios measured in E-MORB from Macquarie Island, Famous and popping rock locations. These samples are free of seawater contaminants (text) but the outlying I/Cl ratios are ascribed to palagonite contamination (see Fig 5b). The range of mantle K/Cl is poorly defined and the grey box is 'open' to higher K/Cl in part 'b'.

Fig 5 (Kendrick et al., 2013)
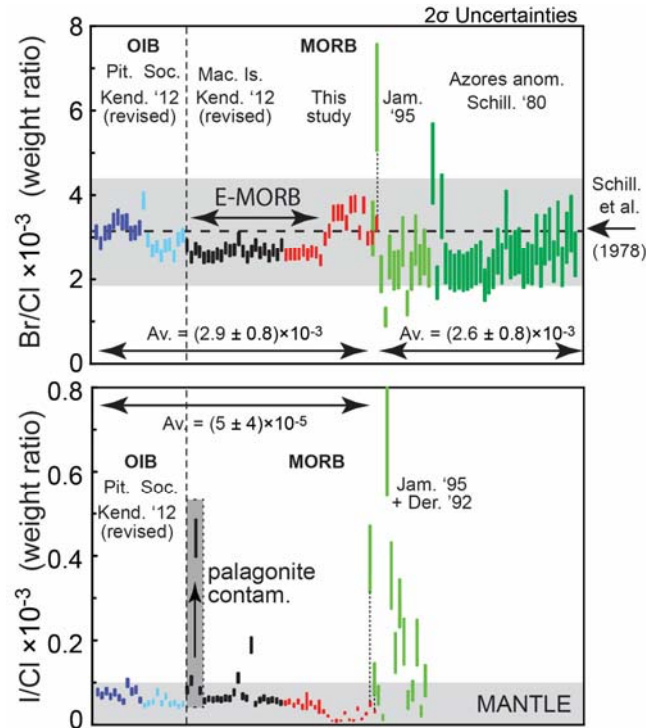
Fig 5. Br/Cl and I/Cl data obtained for basalt glasses using the noble gas method (this study; (Kendrick et al., 2012a; Kendrick et al., 2012b) and radiochemical neutron activation analyses in previous studies (Deruelle et al., 1992; Jambon et al., 1995; Schilling et al., 1978; Schilling et al., 1980). The noble gas data are assigned 2σ uncertainties of 5% for Br/Cl and 10 % for I/Cl that reflect the reproducibility of these parameters in the most uniform standard (Fig 1). The RNAA Br/Cl data is assigned a 2σ uncertainty of 20% (Unni and Schilling, 1977), but uncertainties of 10-40%, based on the I measurement are shown for I/Cl (Deruelle et al., 1992). E-MORB has strikingly uniform Br/Cl and I/Cl; the highest I/Cl ratios are attributed to palagonite contamination that affect different aliquots of a single sample (47979; highlighted in dark grey box) to different extents (see text).
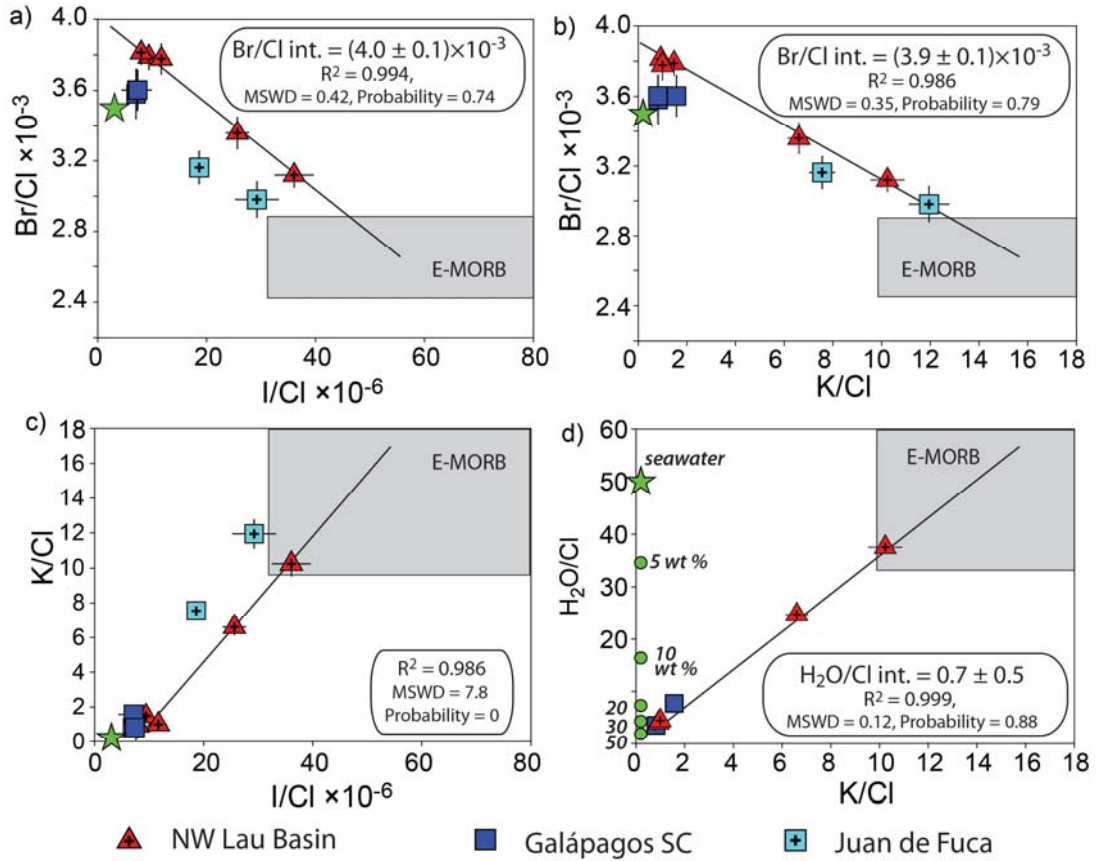
Fig 6 (Kendrick et al., 2013)

Fig 6. Halogen, H$_2$O and K systematics of samples contaminated by seawater-derived components (H$_2$O data are from Perfit et al. (1999) and Lytle et al. (2012). The composition of seawater is shown as a star in each panel. An interpreted mixing line is shown through samples from the northwest part of the Lau Basin (NW Lau Spreading Centre and Rochambeau Rifts) with statistics defining the quality of fit (statistical regressions were performed using Microsoft Excel and the Isoplot program (Ludwig, 2009)). Note that brine salinities are shown in italicised bold labels on the H$_2$O/Cl axis in part d. The H$_2$O/Cl of the brine (e.g. salinity) depends on the K/Cl of the brine and is estimated as 55 ± 15 wt. % salts (see text and Table 2).
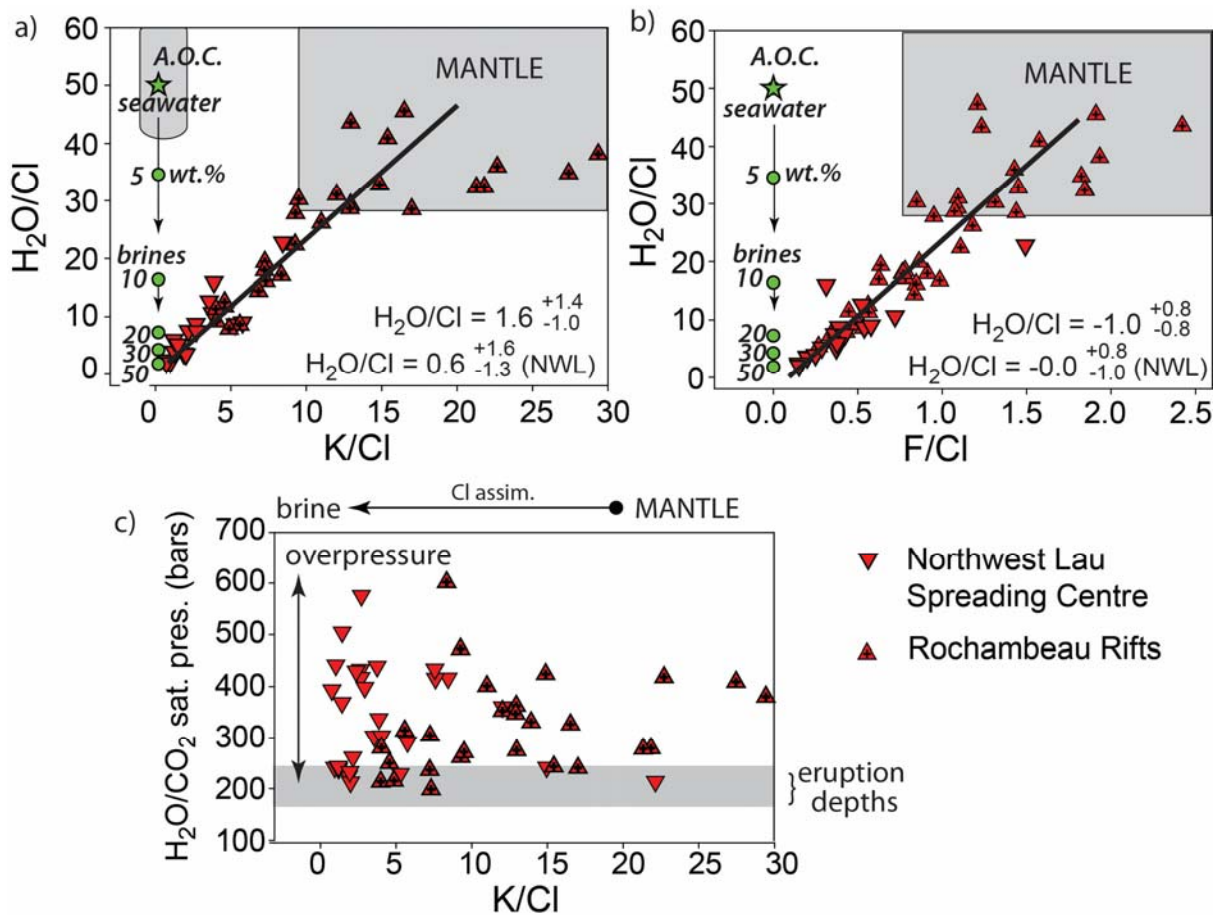
Fig 7 (Kendrick et al., 2013)

Fig 7. Recently published ion-microprobe data for melts from the northwest part of the Lau Basin (Lytle et al., 2012): H_2O/Cl versus a) K/Cl and b) F/Cl showing the trends identified in Fig 6 are regionally significant. The regression uncertainties are 2σ and were obtained using 'robust regressions' in the Isoplot program (Ludwig, 2003). In each case regressions are shown for all data and data from the North West Lau Spreading Centre (NWL) only. Note than Altered Ocean Crust (A.O.C.) has higher H_2O/Cl than unaltered rocks and low K/Cl (Ito et al., 1983; Sano et al., 2008). c) saturation pressure calculated from H_2O and CO_2 concentrations reported in Lytle et al (2012) using the VolatileCalc program (Newman and Lowenstern, 2002).
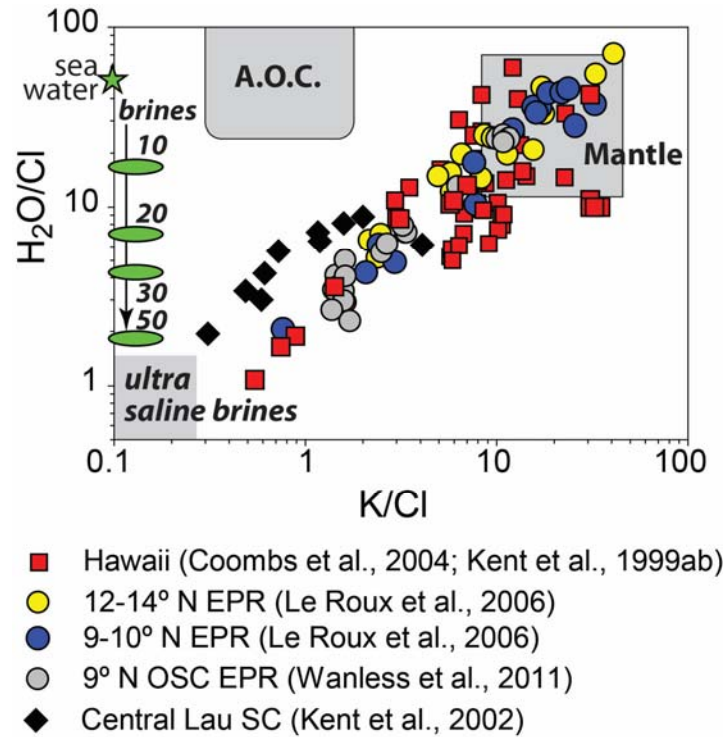
Fig 8 (Kendrick et al., 2013)

Fig 8. Chlorine, H₂O and K data for samples investigated in previous studies (log scale; Coombs et al., 2004; Kent et al., 1999ab;2002; Le Roux et al., 2006;Wanless et al., 2011). Altered ocean crust (AOC) has variable composition but is estimated to have higher H_2O/Cl than unaltered rocks (and in most cases seawater) and K/Cl of 0.3-2 (Ito et al. 1983; Sano et al., 2009); seawater and brines with salinities of 5, 10, 20, 30 and 50 wt % salts are shown for reference. The data are all interpreted as lying on mixing lines between mantle reservoirs with K/Cl of ~7-30 and H_2O/Cl of 10-60; and an ultra-saline brine with H_2O/Cl of <1.6. As originally identified by Michael and Schilling (1989), assimilation of altered ocean crust cannot explain Cl over enrichment.
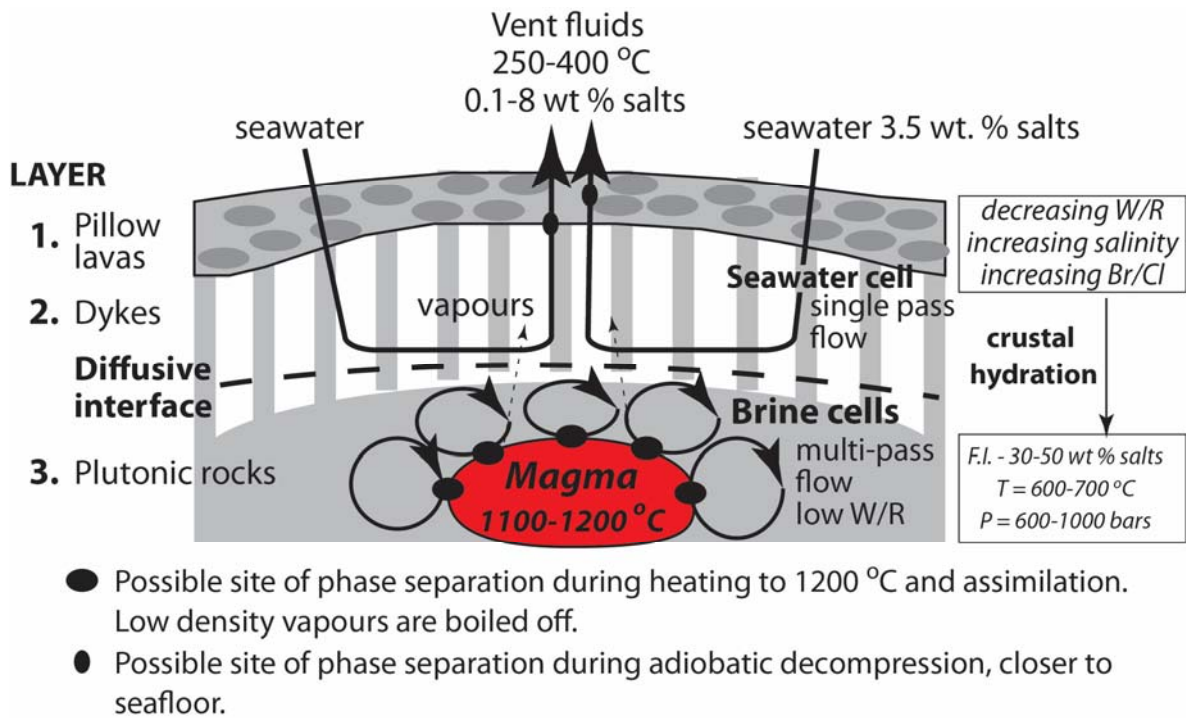
Fig 9 (Kendrick et al., 2013)

Fig 9. Conceptual model for brine circulation at a spreading centre modified after Bischoff and Rosenbauer (1989). Seawater is drawn into the crust where it begins to hydrate the crust and is heated. Preferential incorporation of $OH^->Cl^->Br^-$ into hydrous minerals increases the salinity and Br/Cl of the fluids. Fluids coming into direct contact with magmas via a 'cracking front' or deeply penetrating faults are super-heated with vapours boiled off and brines either retained in the deep crust or assimilated by the magma. Long term trapping of brine is demonstrated by the prevalence of low salinity vent fluids (e.g. Endeavour Field, Juan de Fuca Ridge; Seyfried et al., 2003), and the high Br/Cl of brine-contaminated melts (Figs 4 and 6). Fluid inclusions (F.I.) in quartz veins associated with Cl-rich amphibole in greenschist and amphibolite facies gabbros have salinities of ~50 wt % salt and trapping temperatures of 600-700 °C (Vanko, 1986; 1988). W/R denotes water/rock.
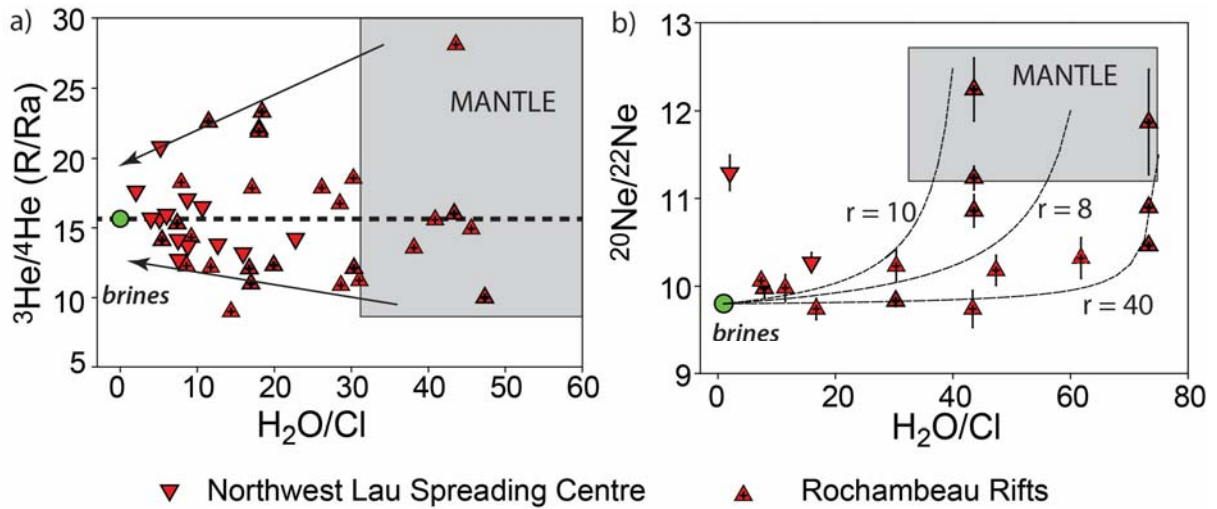
Fig 10 (Kendrick et al., 2013)

Fig 10. Noble gas versus H₂O/Cl plots used to assess the possible role of brine assimilation in altering noble gas signatures. The mean $^3He/^4He$ ratio of 15.4 R/Ra is shown as a dashed line in part a. The r-values in part b define the curvature of the proposed mixing trends where r = $(^{22}Ne/Cl)_{brine}/(^{22}Ne/Cl)_{mantle}$ (Langmuir et al., 1978).